

RESEARCH ARTICLE

10.1002/2015JG003062

Key Points:

- Large uncertainty exists in estimates of terrestrial NPP and NBP in China
- Methodological differences greatly contribute to the uncertainty in NPP and NBP
- Uncertainty in the interannual pattern of NBP is greater than that of NPP

Supporting Information:

- Supporting Information S1
- Table S1
- Table S2
- Table S3
- Table S4
- Table S5
- Table S6
- Table S7
- Table S8
- Table S9
- Table S10
- Table S11
- Table S12
- Table S13
- Data Set S1
- Data Set S2
- Data Set S3
- Data Set S4
- Data Set S5
- Data Set S6
- Data Set S7
- Data Set S8
- Data Set S9
- Data Set S10
- Data Set S11
- Data Set S12
- Data Set S13
- Data Set S14
- Data Set S15
- Data Set S16
- Data Set S17

Correspondence to:

X. Zhou,
xhzhou@des.ecnu.edu.cn

Citation:

Shao, J., et al. (2016), Uncertainty analysis of terrestrial net primary productivity and net biome productivity in China during 1901–2005, *J. Geophys. Res. Biogeosci.*, 121, doi:10.1002/2015JG003062.

Received 21 MAY 2015

Accepted 12 APR 2016

Accepted article online 28 APR 2016

Uncertainty analysis of terrestrial net primary productivity and net biome productivity in China during 1901–2005

Junjiong Shao^{1,2}, Xuhui Zhou^{1,3}, Yiqi Luo⁴, Guodong Zhang², Wei Yan⁵, Jiaxuan Li⁵, Bo Li², Li Dan⁶, Joshua B. Fisher⁷, Zhiqiang Gao⁸, Yong He⁹, Deborah Huntzinger¹⁰, Atul K. Jain¹¹, Jiafu Mao¹², Jihua Meng¹³, Anna M. Michalak¹⁴, Nicholas C. Parazoo^{7,15}, Changhui Peng^{16,17}, Benjamin Poulter¹⁸, Christopher R. Schwalm¹⁹, Xiaoying Shi¹², Rui Sun²⁰, Fulu Tao^{8,21}, Hanqin Tian²², Yaxing Wei¹², Ning Zeng²³, Qian Zhu¹⁷, and Wenquan Zhu²⁴
¹State Key Laboratory of Estuarine and Coastal Research, Tiantong National Field Observation Station for Forest Ecosystem, School of Ecological and Environmental Sciences, East China Normal University, Shanghai, China, ²Coastal Ecosystems Research Station of Yangtze River Estuary, Ministry of Education Key Laboratory for Biodiversity Science and Ecological Engineering, Institute of Biodiversity Science, School of Life Sciences, Fudan University, Shanghai, China, ³Center for Global Change and Ecological Forecasting, East China Normal University, Shanghai, China, ⁴Department of Microbiology and Plant Biology, University of Oklahoma, Norman, Oklahoma, USA, ⁵Shanghai Key Laboratory for Urban Ecological Processes and Eco-Restoration, East China Normal University, Shanghai, China, ⁶Institute of Atmospheric Physics, Chinese Academy of Sciences, Beijing, China, ⁷Jet Propulsion Laboratory, California Institute of Technology, Pasadena, California, USA, ⁸Institute of Geographical Sciences and Natural Resource Research, Chinese Academy of Sciences, Beijing, China, ⁹National Climate Center, China Meteorological Administration, Beijing, China, ¹⁰School of Earth Sciences and Environmental Sustainability, Northern Arizona University, Flagstaff, Arizona, USA, ¹¹Department of Atmospheric Sciences, University of Illinois at Urbana-Champaign, Urbana, Illinois, USA, ¹²Climate Change Science Institute and Environmental Sciences Division, Oak Ridge National Laboratory, Oak Ridge, Tennessee, USA, ¹³Institute of Remote Sensing and Digital Earth, Chinese Academy of Sciences, Beijing, China, ¹⁴Department of Global Ecology, Carnegie Institution for Science, Stanford, California, USA, ¹⁵Joint Institute for Regional Earth System Science and Engineering, University of California, Los Angeles, California, USA, ¹⁶Institute of Environmental Sciences, University of Quebec at Montreal, Montreal, Quebec, Canada, ¹⁷Laboratory for Ecological Forecasting and Global Change, College of Forestry, Northwest A&F University, Yangling, China, ¹⁸Department of Ecology, Montana State University, Bozeman, Montana, USA, ¹⁹Woods Hole Research Center, Falmouth, Massachusetts, USA, ²⁰State Key Laboratory of Remote Sensing Science, School of Geography and Remote Sensing Science, Beijing Normal University, Beijing, China, ²¹Natural Resources Institute Finland (Luke), Vantaa, Finland, ²²International Center for Climate and Global Change Research, School of Forestry and Wildlife Sciences, Auburn University, Auburn, Alabama, USA, ²³Department of Atmospheric and Oceanic Science and Earth System Science Interdisciplinary Center, University of Maryland, College Park, Maryland, USA, ²⁴State Key Laboratory of Earth Surface Processes and Resource Ecology, Beijing Normal University, Beijing, China

Abstract Despite the importance of net primary productivity (NPP) and net biome productivity (NBP), estimates of NPP and NBP for China are highly uncertain. To investigate the main sources of uncertainty, we synthesized model estimates of NPP and NBP for China from published literature and the Multi-scale Synthesis and Terrestrial Model Intercomparison Project (MsTMIP). The literature-based results showed that total NPP and NBP in China were 3.35 ± 1.25 and 0.14 ± 0.094 Pg C yr⁻¹, respectively. Classification and regression tree analysis based on literature data showed that model type was the primary source of the uncertainty, explaining 36% and 64% of the variance in NPP and NBP, respectively. Spatiotemporal scales, land cover conditions, inclusion of the N cycle, and effects of N addition also contributed to the overall uncertainty. Results based on the MsTMIP data suggested that model structures were overwhelmingly important (>90%) for the overall uncertainty compared to simulations with different combinations of time-varying global change factors. The interannual pattern of NPP was similar among diverse studies and increased by 0.012 Pg C yr⁻¹ during 1981–2000. In addition, high uncertainty in China's NPP occurred in areas with high productivity, whereas NBP showed the opposite pattern. Our results suggest that to significantly reduce uncertainty in estimated NPP and NBP, model structures should be substantially tested on the basis of empirical results. To this end, coordinated distributed experiments with multiple global change factors might be a practical approach that can validate specific structures of different models.

1. Introduction

As a consequence of increasing atmospheric carbon dioxide (CO_2) concentration, global air temperature has risen by 0.85°C during 1880–2012 and is predicted to increase by another 0.3 – 4.8°C by the end of this century [Intergovernmental Panel on Climate Change, 2013]. The global warming may substantially affect the global carbon (C) cycle, leading to a positive or negative feedback to climate change [Friedlingstein et al., 2006; Heimann and Reichstein, 2008]. Global terrestrial ecosystems are estimated to absorb about 30% of the anthropogenic CO_2 emissions, which considerably mitigate climate change, especially global warming [Canadell et al., 2007b; Le Quéré et al., 2014]. The mitigation ability of ecosystems is determined by net biome productivity (NBP), which is net primary productivity (NPP) minus heterotrophic respiration (Rh) and fire flux ($\text{NBP} = \text{NPP} - \text{Rh} - \text{fire flux}$) when latent and non- CO_2 fluxes can be omitted [Chapin et al., 2006; Fisher et al., 2014]. Both NPP and NBP are important components of the global C cycle and are used as indicators of ecosystem function, which are closely related to biodiversity, biogeochemical cycling, ecosystem resilience, and other aspects of ecosystem services [Canadell et al., 2007a; Richamond et al., 2007; Ito, 2011]. Therefore, estimating the magnitudes of NPP and NBP is critical for evaluating global and regional ecosystem services and providing a scientific basis for international climate change negotiations and is therefore of great importance to all human beings as well as to policy makers.

Unfortunately, current estimates of NPP and NBP at global and regional scales are highly uncertain. For example, the uncertainty (referred to as coefficient of variation (CV)) in global NPP and NBP among different studies was 25% and 151%, respectively [Ito, 2011] (Table S10 in the supporting information), while those in China, conterminous United States (U.S.), and Europe were 37%, 31%, and 11%, respectively, for NPP and 67%, 106%, and 42% for NBP (Tables S1, S2, and S11). At best, global and regional estimates of NPP are given within an order of magnitude among studies (e.g., the estimated NPP in Europe was 2.97 – $4.12 \text{ Pg C yr}^{-1}$ (minimum–maximum) [Jung et al., 2007]), while the difference in NBP could be as high as 40-fold for global estimates (-0.42 – $17.1 \text{ Pg C yr}^{-1}$ [McGuire et al., 2001; Jung et al., 2011]) (Figure S1 in the supporting information). Given the level of uncertainty, it is hard to differentiate NPP or NBP among China, Europe, and the U.S. Large uncertainties in NPP and NBP among estimates may be attributed to several sources: (1) differences in the choice of driving data used in process-based models [Rivington et al., 2006]; (2) different flux component attributions of NBP among atmospheric inversion, inventory, and forward model approaches [Hayes et al., 2012]; (3) discrepancies in model structure, which includes model assumptions, spatiotemporal resolution, and parameter values [Cramer et al., 1999; Gurney et al., 2003]; (4) inconsistency of study periods in intercomparisons due to high interannual variability (IAV) in C fluxes [Baldocchi, 2008; Le Quéré et al., 2009]; and (5) whether the effects of global change factors were included or not [Tian et al., 2011a; Bouskill et al., 2014]. Identifying how these aspects influence the uncertainty in estimates of regional NPP and NBP is essential in order to improve predictions of terrestrial C cycle–climate feedback.

As one of the biggest countries with an area of $960 \times 10^6 \text{ ha}$, China significantly contributes to the global CO_2 emissions and has become the largest emitter since 2006 [Gregg et al., 2008]. The total CO_2 emission in China accounts for 27% of global emission, about twice of the second largest emitter (the U.S.). The growth rate of CO_2 emissions (1.2% from 2013 to 2014) in China is the second largest emitters (Indian 8.6%, U.S. 0.8%, and Europe -5.8%) [Le Quéré et al., 2015]. In order to fulfill its international obligations, China's government has promised to reduce its CO_2 emissions by 40–45% per unit of gross domestic product by 2020 compared with 2005, which requires the electric power departments to constrain their CO_2 emissions, as well as the development of new and renewable energy sources [Wang et al., 2015]. Meanwhile, China's government is attempting to optimize the managements of forests and croplands for C sequestration [Deng et al., 2009; Zhao et al., 2012]. Whether China can effectively contribute to the mitigation of global warming depends on the magnitude of net C balance, which highlights the need to study terrestrial NPP and NBP intensively in China. To date, more than 600 papers have been published in English (Web of Science) or Chinese (China National Knowledge Infrastructure), focusing on NPP or NBP at spatial scales from individual ecosystems to the whole country (the search terms were described in section 2.1). Despite the efforts being made, the differences among the estimations are as large as several times for NPP (1.43 – $7.44 \text{ Pg C yr}^{-1}$ [Chen et al., 2001; Piao et al., 2005]) and tens of times for NBP (0.017 – $0.35 \text{ Pg C yr}^{-1}$ [Ren et al., 2007; Piao et al., 2009a]).

The large uncertainty in the estimated NPP and NBP of China's terrestrial ecosystems may result from methodological differences (especially differences among models in terms of flux attributions, assumptions,

structure, inputs, and performance) [Gao and Liu, 2008; Piao et al., 2009a], which has led to an uncertainty (CV) of 12–39% in NPP [Dan et al., 2007; Gao and Liu, 2008; Mao et al., 2010] and 23% in NBP [Piao et al., 2009a] for the recent decades. The uncertainty may also be augmented by the IAV in NPP and NBP. For example, Tao and Zhang [2010] showed the increasing trends for both NPP and NBP since the 1930s, resulting in higher estimates in the later period than those in the earlier period. The different choice of time periods in diverse studies may cause inconsistent estimations for NPP and NBP. In addition, the different models may simulate or predict diverse spatial patterns of NPP and NBP, especially in areas with heterogeneous topography and/or vegetation. For example, Gao and Liu [2008] demonstrated that the Geo-Process Model-Based Ecosystem Photosynthesis Theory model estimated the lowest NPP in Inner Mongolia among five models, but it showed a relatively high NPP in the Qinghai-Tibet region. Therefore, quantifying the uncertainty in the estimated NPP and NBP and identifying the main sources are essential for accurately estimating NPP and NBP in the future.

In this study, we compiled and synthesized published NPP and NBP data in China's terrestrial ecosystems over the past 30 years to assess their uncertainty and attribution, especially from differences in methods and spatiotemporal variability. Among diverse methods, we examined the proportion of uncertainty introduced by different model types, drivers, spatiotemporal resolutions, and data. For temporal patterns, we investigated whether different models showed consistent temporal patterns and the relative importance of climatic drivers to the IAV in NPP and NBP. For spatial patterns, we assessed the uncertainty in NPP and NBP at the grid and biome scales and compared the estimated NPP and NBP and uncertainty between China and other regions (Africa, conterminous U.S., and Europe). Besides the data from published literature, we also analyzed model output from the North American Carbon Program (NACP) Multi-scale Synthesis and Terrestrial Model Intercomparison Project (MsTMIP) [Huntzinger et al., 2013; Wei et al., 2014]. The MsTMIP models were run using a common set of driver data and a common protocol and included a series of sensitivity analyses, which provided an opportunity to confirm the literature-based results and compare the relative importance of model structures with influences of time-varying forcing drivers. The objectives of this work are to quantify the uncertainty of the estimated NPP and NBP, identify the primary sources of uncertainty, and compare the mean values and their uncertainty in China with those in other areas and the world.

2. Materials and Methods

2.1. Data Sources

Peer-reviewed published papers were searched using Web of Science (www.webofknowledge.com) for English papers and China National Knowledge Infrastructure (www.cnki.net) for Chinese papers (1980–2011). The key words were restricted to gross primary producti*, net primary producti*, respiration, net ecosystem producti*, net ecosystem exchange, net CO₂ exchange, carbon budget, carbon sink, carbon flux, greenhouse gas, and their abbreviations. For English papers, “China” was used as another key word to restrict the study region. Of these papers, only studies meeting the following criteria were selected: First, the study contained the desired variables, including gross primary productivity (GPP), net primary productivity (NPP), ecosystem respiration (RE), soil respiration, autotrophic respiration (Ra), heterotrophic respiration (Rh), net ecosystem productivity (NEP), and net biome productivity (NBP). NEP is the net balance between GPP and RE or between NPP and Rh; NBP is NEP minus the flux caused by disturbance (especially fire, NBP = NEP – fire flux) if latent and non-CO₂ fluxes can be omitted (0.012 and 0.011 Pg C yr^{–1}, respectively [Piao et al., 2009a; Chen et al., 2013]), which indicates the C uptake or source by terrestrial ecosystems [Chapin et al., 2006; Fisher et al., 2014]. Other terms were also used to quantify the ability of ecosystems to sequester C from the atmosphere, such as net ecosystem exchange, net CO₂ exchange, and net C balance, as well as NEP. Although these terms represent different flux components in the absolute sense, they approximate each other when the minor fluxes (fire, latent, and non-CO₂ fluxes) can be ignored [Chapin et al., 2006]. The fire flux (the difference between NBP and NEP when latent and non-CO₂ fluxes are negligible) might be critical in the fire-induced ecosystems, but its magnitude is very uncertain. Moreover, the results based on inventory and remote sensing data suggested that this fire flux in China could be neglected (~0.01 Pg C yr^{–1}) [Tian et al., 2003; Lü et al., 2006]. Therefore, the studies that considered NEP as an indicator of the C sink in China may be valid. For convenience, we used NBP to generally represent

all these terms, but we discussed the difference between NBP and NEP in relevant context. Second, the study reported total fluxes across the China or a certain biome of China (forest, shrubland, grassland, or cropland), not an individual ecosystem.

For completeness, we fully surveyed the citations of the obtained papers and collected the ones meeting the criteria above. We then extracted the desired annual C fluxes, including time series data (during 1981–2000) and summaries (in any period during 1901–2005), as well as climatic variables (radiation, temperature, precipitation, and CO₂ concentration for 1981–2000) and biome area. However, most studies did not report the synchronous climatic variables, and we only obtained one, seven, seven, and three time series data sets for radiation, temperature, precipitation, and CO₂ concentration, respectively. Because some original climate data are anomalies rather than the absolute values, all the original climatic data were first transformed to anomalies, averaged among studies, and then were normalized by subtracting the mean and being divided by the standard deviation (SD) of multiple-year data. We also directly contacted the authors for spatial NPP data and obtained 16 digital maps from Sun and Zhu [2000], He et al. [2005], Meng et al. [2005], Dan et al. [2007], Zhu et al. [2007a], Gao and Liu [2008], and Tao and Zhang [2010]. Although the comparison between model outputs and the observed site-level data is difficult and beyond the scope of our study, we still extracted the field observed NPP of certain ecosystem types from literature and the eddy-flux NEP data from ChinaFLUX [Yu et al., 2013] in order to complete our information on the C fluxes of China's terrestrial ecosystems.

In total, the literature-based data sets covered from 1901 to 2005 and the durations of these studies ranged from 1 to 102 years, with most studies focusing on the last two decades of the 20th century. There were 54 estimates of China's NPP and 14 of NBP, while the estimates of the other fluxes were relatively scarce. For those data from the main biomes in China, there were 90 and 34 estimates of NPP and NBP, respectively. Despite the different criteria used for forest type classification among studies, we classified the forest biome into evergreen needleleaf forest (ENF), evergreen broadleaf forest (EBF), deciduous needleleaf forest (DNF), deciduous broadleaf forest (DBF), and mixed forest (MF). There were in total 189 NPP estimates for these subtypes of forests.

In addition to the published literature, the Multi-scale Synthesis and Terrestrial Model Intercomparison Project (MsTMIP) [Huntzinger et al., 2013; Wei et al., 2014] conducted by the North American Carbon Program (NACP) provides a great opportunity to compare the results among the models with a common driving data set, in which the MsTMIP models were run by both constant and varying drivers. Therefore, we extracted China's NPP, NEP, and NBP data from the global maps of 14 of the models available as part of the MsTMIP Version 1.0 release (<http://nacp.ornl.gov/mstmipdata/>, [Huntzinger et al., 2015]; CLASS-CTEM-N was not included because its NPP estimate of China was 0.51 Pg C yr⁻¹, an order of magnitude lower than what is thought to be a reasonable estimate), and conducted a parallel analysis to the literature-based data. We selected the time period of 1981–2000 for MsTMIP data, because the majority of the literature focused on this period.

2.2. Covariates

For a given variable, the mean \pm SD and the coefficient of variation (CV) were used to represent the uncertainty among models. To investigate the potential sources of uncertainty in the NPP and NBP of China, the data were grouped according to the types of methods, spatiotemporal resolution, the inclusion of global change factors (climate change (warming and altered precipitation), elevated atmospheric CO₂ and O₃ concentration, N addition, fire, and land cover and land use change (LCLUC)), the types of biomes, and subtypes of forests.

The methods used to estimate regional C fluxes covered a series of approaches [Hayes et al., 2012; Fisher et al., 2014], which can be broadly classified into top-down (i.e., atmospheric inversions) and bottom-up approaches. The bottom-up approach includes biomass inventory and forward model approaches; the latter in turn contains statistical (e.g., Miami and Thornthwaite Memorial models) and process models. Based on the methods to simulate the GPP or NPP, the process models can be further grouped into light use efficiency (LUE) and enzyme kinetics (EK) models [e.g., Huntzinger et al., 2012]. In our study, the methods of estimating NPP included statistical model, LUE model, EK model, and a combination of multiple models (when a study reported only the grand mean of several models rather than individual outputs). The LUE models were further classified into LUE_GPP and LUE_NPP when the former had and the latter did not have an

independent Ra module, respectively. For NBP, the estimated methods included the atmospheric inversion model, the inventory method, the process model, and a combination of multiple models. The features of these models have been well documented by *Cramer et al.* [1999], *Adams et al.* [2004], *Schwalm et al.* [2010], and *Huntzinger et al.* [2013].

The temporal scale was categorized into short (subdaily), median (weekly or 10 days), and long (monthly or longer). The spatial scale was partitioned into fine (1–4 km), median (8–10 km or 0.1°), and coarse (50 km or larger than 0.5°). We treated the spatiotemporal scales as ordered category variables instead of numerical in this study based on two considerations. First, although the scales are numerical values, in practice only a few spatiotemporal scales were numerically used according to the data sources and model structures. Second, the extremely small sample sizes for the beginnings and ends of the spatiotemporal scales may lead to the biased results because the classification and regression tree (CART, see section 2.3) only considered the rank orders of the numeric explanatory variables. Prescribed groups of spatiotemporal scales can partly dismiss such biases. The process models were further dichotomized according to whether they considered global change factors (e.g., climate change, CO₂, O₃, N addition, fire, and LCLUC) or not. In addition, we obtained or calculated estimations for the effects of global change factors on China's NPP and NBP according to the reported results of different scenarios.

2.3. Classification and Regression Tree

The classification and regression tree (CART) [Breiman et al., 1984] was applied to partition and identify the contributions of different sources to the ultimate intermodel uncertainty in NPP and NBP of China. The CART is a nonparametric statistical method that is ideally suited for the analysis on complex data structures involving nonnormality, heterogeneous of variance, unbalanced sample sizes, and missing values [De'ath and Fabricius, 2000]. It is able to incorporate nonlinear relationships and to quantify the relative importance of each factor to the total variance of the response variable. The logic of CART is to maximize the overall homogeneity of the tree (here maximize the between-group variations and minimize within-group variations) by sequentially splitting the data into two groups. At each step, from all possible splits of all explanatory variables, the CART selects the one to maximize the homogeneity as the primary split, which is usually presented in a CART diagram [De'ath and Fabricius, 2000]. However, other unchosen variables could also be important, which can be quantified according to their relative improvements compared with the primary split. As a result, the relative contribution of each explanatory variable to the overall variance of the response variable is derived across all the possible splits.

The CART was applied to the literature-based and MsTMIP data sets, separately, because the MsTMIP models were driven by a common data set, while the covariates corresponding to literature-based data were more variable. The choices of explanatory variables for the CART models were based on the available data. The explanatory variables for the literature-based NPP included model type, spatial scale, temporal scale, inclusion of the N cycle, CO₂ effect and LCLUC (presence or absence), land cover condition (uniform or heterogeneous), and type of driving data (remotely sensed or field observed meteorological data), while those for the literature-based NBP included model type, spatial scale, temporal scale, inclusion of the N cycle, LCLUC, N addition and fire effects, land cover condition, and type of driving data. Note that the inclusion of climatic variations was not regarded as an explanatory variable, because all the models included this effect except for the studies that only focused on a single year. In addition, the inclusion of CO₂ and O₃ effects was not considered as an explanatory variable for the literature-based NBP data, because all the process models considered the CO₂ fertilization, and the models that included O₃ effects were those that also included N addition effects. However, the relative importance of climatic variations and CO₂ fertilization to the intermodel uncertainty can be quantified by analyzing the MsTMIP data. The O₃ effects might not be important according to current model outputs [Ren et al., 2007; Tian et al., 2011a].

The MsTMIP models were run using a consistent set of environmental driving data for a series of sensitivity simulations that add one time-varying driver at a time to test the influences of four key forcing factors: climate, land cover change, atmospheric CO₂ concentration, and nitrogen deposition. Therefore, the MsTMIP experimental design isolates the impact of model structure (i.e., process inclusion and formulation) on modeled results. The sensitivity simulations enable us to quantify the relative importance of diverse model structures and time-varying global change factors to the overall ensemble spread of uncertainty. To evaluate the influence of fire effect on total uncertainty, we also calculated the NBP estimates without fire effects (i.e.,

NEP estimates) for the four models that had a fire module (Biome-BGC, CLM4, CLM4VIC, and TEM6), in addition to their original estimates of NBP in different simulations. As a result, the CART was applied on all the possible combinations of models, simulations, and inclusion of fire effects (totally 78 realizations of land carbon flux; Table S3). The explanatory variables were model identity (a categorical variable indicating which model was used), which time-varying driver was used to drive the simulations (i.e., climatic variations, LCLUC, CO₂ enrichment, and N addition) and whether the fire effect was included. The *rpart* function from the R package *rpart* was used to conduct the CART analysis [Therneau et al., 2015].

2.4. Interannual Variability

To test whether the patterns of IAV in NPP and NBP were consistent among studies, the repeated measures analysis of variance (RMANOVA) was applied to the collected time series during 1981–2000 both for the literature-based and MsTMIP data sets. We applied the RMANOVA with the repeated measured factor (year) but no group factor, because our focus was on the interannual pattern rather than the magnitude of NPP and NBP. The RMANOVA is aimed to test the differences among repeated measures (the year in this case) after excluding the influence of subjects (here models) [Gravetter and Wallnau, 2007]. Therefore, if the effect of a repeated measures factor (year) was statistically significant ($p < 0.05$), the interannual patterns could be regarded as consistence among the models. To quantify the relative importance of the climatic variables to the IAV in C fluxes during 1982–1999 (the radiation data in 1981 and 2000 were missing, so the analysis can only be conducted on this period), we fitted multiple linear regression models ($\text{Flux} = b_0 + b_1 \times \text{Radiation} + b_2 \times \text{Temperature} + b_3 \times \text{Precipitation} + b_4 \times \text{CO}_2$). The Lindeman-Merenda-Gold (LMG) values [Lindeman et al., 1980] were also calculated to provide a decomposition of the models explained variance [Bi and Chung, 2011]. These represent the relative importance of each variable to the total temporal variance in C fluxes. In multiple regression models, the sequential r^2 (Type I sums of squares) depends on the order of the regressor. The LMG value of a variable is the mean sequential r^2 obtained by averaging over all possible orderings. The *calc.relimp* function from the R package *relaimpo* was used to calculate the LMG values [R Core Team, 2013].

2.5. Spatial Patterns

To investigate the uncertainty in the spatial patterns of the literature-based NPP estimates among the models, the digital maps were first resampled to a 10 km \times 10 km resolution. Every pixel's NPP in a resampled map was rescaled using the formula $(x - \min(x)) / \text{range}(x)$, where x is the NPP in the map. As a result, the differences among models caused by the NPP magnitude were eliminated, and the rescaled values were between 0 and 1 for the minimum and maximum data in China, respectively. The SD of the rescaled NPP in a certain pixel among maps was calculated as the indicator of the uncertainty in the spatial pattern. Specifically, a small SD in a certain area suggests that the models agree with each other in the terms of their spatial patterns, whereas a large SD suggests great uncertainty. The SD was also calculated based on the MsTMIP NPP and NBP digital maps, except that the maps were not resampled because the original spatial resolution of the MsTMIP outputs was all 0.5 by 0.5°.

3. Results

3.1. Magnitude, Uncertainty, and Interannual Variability of the NPP and NBP in China

According to the literature-based data set with 54 NPP estimates from 33 studies, the NPP in China's terrestrial ecosystems was $3.35 \pm 1.25 \text{ Pg C yr}^{-1}$ (mean \pm SD) during 1901–2005 (most estimates were during 1981–2000; Figure 1 and Table S1), which was very close to the value from outputs of the Multi-scale Synthesis and Terrestrial Model Intercomparison Project (MsTMIP) during 1981–2000 ($3.36 \pm 0.63 \text{ Pg C yr}^{-1}$; Figure 1 and Table S3). Classification and regression tree (CART) analysis for the literature-based data set showed that the model type accounted for 36% of the explained variance among NPP estimates from the literature data, with the significant difference between statistical ($4.32 \pm 1.42 \text{ Pg C yr}^{-1}$) and other models ($3.18 \pm 1.37 \text{ Pg C yr}^{-1}$) as the primary source of variance and that between light use efficiency (LUE) and enzyme kinetics (EK) models as the secondary contributor (Figure 2). In order of importance, the other sources of uncertainty were the temporal scale (23%), land cover condition (14%), spatial scale (14%), inclusion of the nitrogen (N) cycle (12%), and the type of driving data (1%). For the MsTMIP outputs, some of the uncertainty sources (e.g., the spatiotemporal scales and land cover conditions) were eliminated because the MsTMIP models were run using a common set of

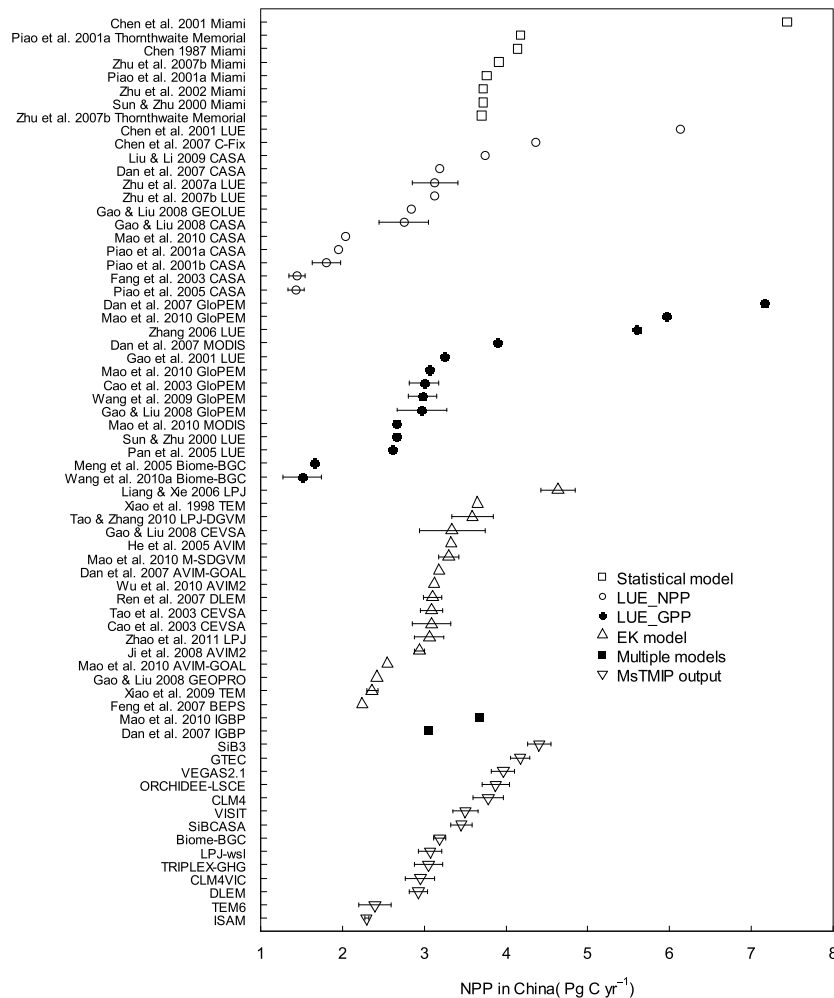


Figure 1. Total net primary productivity (NPP) of China. The error bar is the standard deviation of annual NPP during the study period (i.e., interannual variability). LUE_NPP indicates the models using light use efficiency to simulate NPP; LUE_GPP represents the models using light use efficiency to simulate GPP and other modules to simulate autotrophic respiration (R_a). The references labeled in the y axis can be found in the supporting information.

driving data and a common simulation protocol [Huntzinger *et al.*, 2013], that included a series of sensitivity simulations that were designed to test the influence of global change factors. The CART results on MSTMIP data set showed that the majority (95%) of the overall uncertainty (i.e., spread) within the ensemble came from model structural differences rather than collective model response to various time varying drivers (global change factors; Figure 3).

According to the literature-based data set with 14 NBP estimations from 11 studies, the terrestrial NBP in China was $0.14 \pm 0.097 \text{ Pg C yr}^{-1}$ (during 1901–2005; Figure 6 and Table S2), which was much lower than the results based on MSTMIP outputs ($0.32 \pm 0.35 \text{ Pg C yr}^{-1}$, during 1981–2000; Figure 6 and Table S3). The model type accounted for 64% of the explained variance among NBP estimates from the literature data, in which the significant difference between top-down ($0.31 \pm 0.0020 \text{ Pg C yr}^{-1}$) and bottom-up approaches ($0.12 \pm 0.0048 \text{ Pg C yr}^{-1}$) was the primary source of variance and the difference between process and other methods was the secondary contributor (Figure 7). The inclusion of N addition effects was also important (24%) but other factors had little effect. The results from the outputs of the MSTMIP also showed that the majority of the uncertainty (90%) stemmed from the models rather than different combinations of time-varying global change factors (Figure 8). The exclusion of TRIPLEX outputs (with an estimated NBP 1 order of magnitude larger than other models) reduced the importance of model structures to 67%; however, the influence of model structure still outweighed other factors (Figure 8).

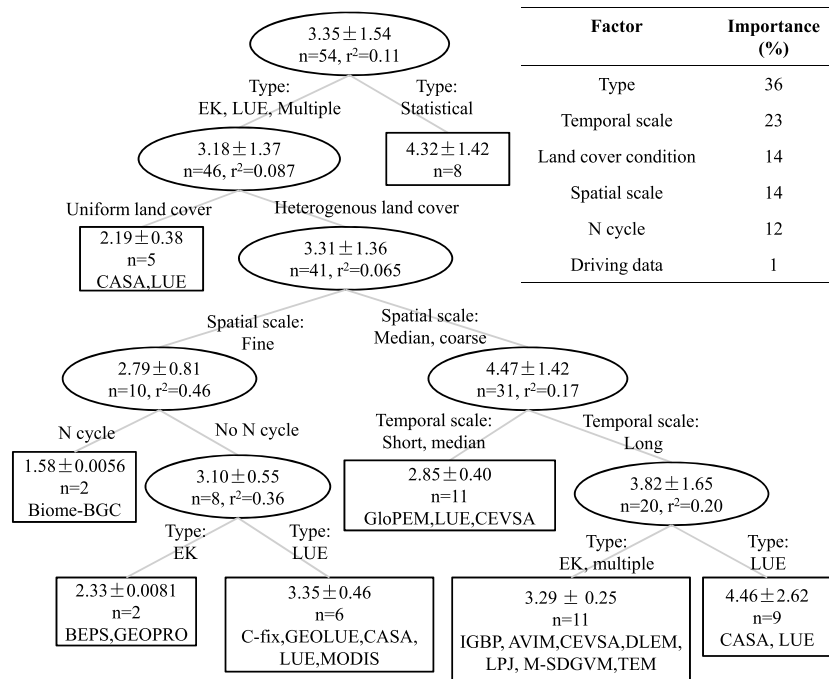


Figure 2. The classification and regression tree (CART) results based on the NPP values from the literature. The values in each node are the estimated mean \pm standard deviation (Pg C yr^{-1}). n , the sample size of tree node; r^2 , the explained proportion of variance of a node by the sequent split.

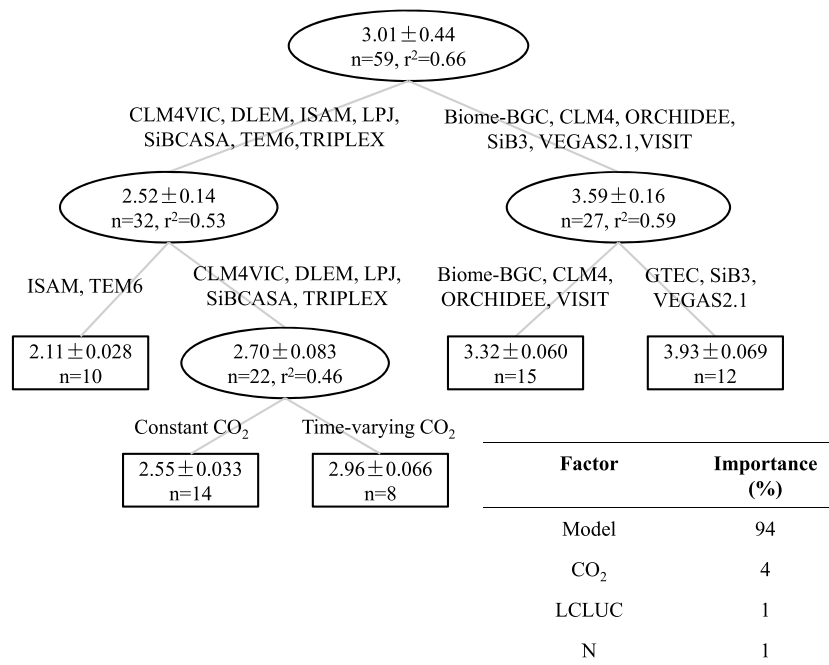


Figure 3. The classification and regression tree (CART) results based on the NPP values from the MsTMIP data set. The values in each node are the estimated mean \pm standard deviation (Pg C yr^{-1}). n , the sample size of tree node; r^2 , the explained proportion of variance of a node by the sequent split.

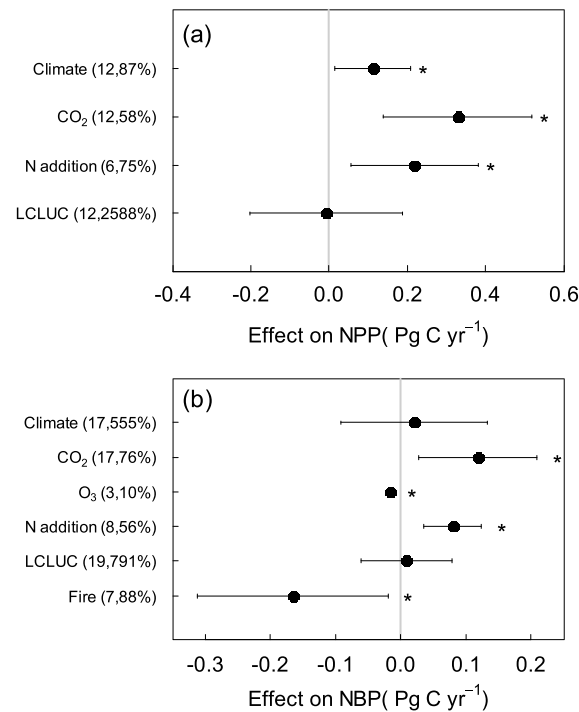


Figure 4. The effects of global change factors on (a) NPP and (b) NBP in China. The error bars represent the SDs. The figures in the parentheses are the sample size and coefficient of variation. The data come from both the literature and MsTMIP data sets. *, significantly different from 0 by *t* test ($p < 0.05$).

Nevertheless, the global change factors could have large effects on the individual model outputs from both the literature and MsTMIP data sets. For example, CO_2 fertilization and N addition largely enhanced both NPP (0.33 ± 0.19 and $0.22 \pm 0.16 \text{ Pg C yr}^{-1}$, respectively, mean \pm SD; Figure 4a) and NBP (0.12 ± 0.09 and $0.079 \pm 0.044 \text{ Pg C yr}^{-1}$, respectively; Figure 4b) in China, whereas the effects of climatic variations and land cover and land use change (LCLUC) were much smaller (Figure 4). The O_3 had a slight negative effect on NBP ($-0.016 \pm 0.0015 \text{ Pg C yr}^{-1}$), while the fire largely decreased the NBP with large uncertainty ($-0.17 \pm 0.15 \text{ Pg C yr}^{-1}$; Figure 4b).

During 1981–2000, China's NPP and NBP fluctuated from year to year. The interannual variability (IAV, in terms of SD) in NPP was 0.07–0.28 and 0.026–0.20 Pg C yr^{-1} for the literature-based and MsTMIP data sets, respectively, while that in NBP was 0.029–0.16 and 0.043–0.19 Pg C yr^{-1} , respectively (Figures 5 and 9). The RMANOVA results showed that the year (the repeated measured factor) significantly contributed to the total variance of annual NPP for the literature-based and MsTMIP data sets (both

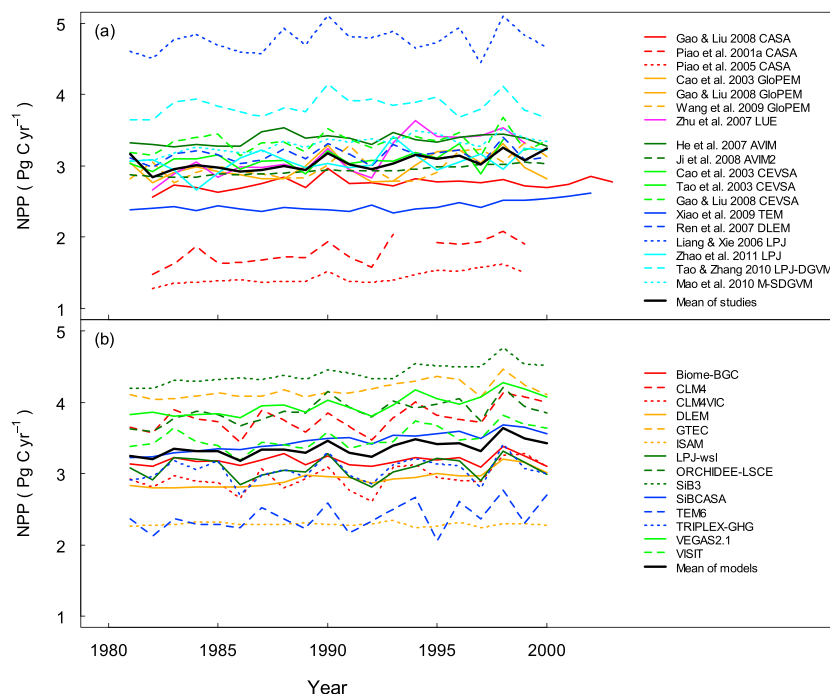


Figure 5. Time series of China's NPP from the (a) literature (1981–2005) and (b) MsTMIP (1981–2000). The references in the legend can be found in the supporting information.

Table 1. The Relative Importance of Radiation, Temperature, Precipitation and CO₂ to the Interannual Variability in Net Primary Productivity (NPP) and Net Ecosystem Productivity (NBP) From the Literature and Multi-scale Synthesis and Terrestrial Model Intercomparison Project (MsTMIP) Outputs^a

	Literature		MsTMIP	
	NPP	NBP	NPP	NBP
Radiation	2%	17%	2%	2%
Temperature	17%	17%	22%	15%
Precipitation	33%	22%	44%	40%
CO ₂	27%	5%	19%	32%
Total r^2	79%	61%	88%	88%

^aThe time series of NPP and NBP were the annual values averaged among models from Figures 5 and 9, respectively. The relative importance metric is the Lindeman-Merenda-Gold (LMG) value of the multiple linear regression model: $\text{Flux} = b_0 + b_1 \times \text{Radiation} + b_2 \times \text{Temperature} + b_3 \times \text{Precipitation} + b_4 \times \text{CO}_2$. Flux represents either NPP or NBP.

$p < 0.001$; Table S4). However, the interannual pattern of NBP among models was inconsistent ($p = 0.31$ and 0.027 for the literature-based and MsTMIP data sets, respectively; Table S4). The relative importance (the LMG value, which provides a decomposition of the model explained variance; see section 2.4) of radiation, temperature, precipitation, and CO₂ to the IAV of the NPP averaged across 18 time series from the literature was 2%, 17%, 33%, and 27%, respectively, which was consistent with the results based on the MsTMIP outputs (Table 1). However,

the relative importance of climatic variables to the IAV in NBP disagreed between the results from the literature and MsTMIP data sets except for the temperature (Table 1).

3.2. NPP and NBP in Different Biomes

Based on the literature data, forests occupy about 20% of China's area ($118\text{--}435 \times 10^6$ ha; Tables S5 and S8). Both the total (0.99 ± 0.56 Pg C yr⁻¹) and mean NPP (640 ± 231 g C m⁻² yr⁻¹) of China's forests were larger than those of other biomes (Figures 10a and 10c). Among the forests, evergreen broadleaf forests (EBF) had the largest mean NPP (729 ± 259 g C m⁻² yr⁻¹), followed by mixed forests (MF, 605 ± 305 g C m⁻² yr⁻¹), evergreen needleleaf forests (ENF, 546 ± 293 g C m⁻² yr⁻¹), deciduous broadleaf forests (DBF, 528 ± 188 g C m⁻² yr⁻¹), and deciduous needleleaf forests (DNF, 431 ± 132 g C m⁻² yr⁻¹), with the uncertainty for all biomes being all above 30% (Figure 10d). Shrublands occupy less than 10% of China's area ($19\text{--}197 \times 10^6$ ha; Tables S5 and S8) and have the lowest NPP (0.30 ± 0.38 Pg C yr⁻¹; Figure 10a), but are not the least productive biome (410 ± 226 g C m⁻² yr⁻¹; Figure 10c). The area of grasslands is about one third of China's total area ($225\text{--}499 \times 10^6$ ha; Tables S5 and S8). Although the mean NPP of grasslands (214 ± 105 g C m⁻² yr⁻¹) was the lowest (Figure 10c), the total NPP was considerable (0.66 ± 0.24 Pg C yr⁻¹; Figure 10a). Croplands occupy about one sixth of China's terrestrial area ($98\text{--}244 \times 10^6$ ha; Tables S5 and S8). The total (0.73 ± 0.30 Pg C yr⁻¹) and mean NPP (495 ± 184 g C m⁻² yr⁻¹) of croplands was just lower than those of forests (Figures 10a and 10b).

Compared to NPP, the estimations of the biomes' NBP were accompanied by much greater uncertainty. The total NBP of forests, shrublands, grasslands, and croplands were 0.073 ± 0.13 , 0.024 ± 0.027 , 0.017 ± 0.011 , and 0.023 ± 0.015 Pg C yr⁻¹, respectively (Figure 10b). The uncertainty in NBP for forests and shrublands (>100%) was much larger than that for grasslands and croplands (both 65%). The relative contributions of these biomes to China's NBP also showed high variability, which were $40 \pm 22\%$, $19 \pm 11\%$, $25 \pm 21\%$, and $18 \pm 15\%$, respectively (Figure 10b).

3.3. Uncertainty in the Spatial Pattern of NPP and NBP

According to the average of the 16 NPP maps derived from the literature and the 14 NPP maps from MsTMIP, the most productive areas were the eastern, southern, and southwestern China, whereas the northwestern China was the least productive (Figures 11a and S1a). The spatial pattern of NBP generally followed that of NPP (Figure S4c). We used the SD of the rescaled NPP and NBP as the indicator of uncertainty in spatial patterns, which eliminated the systematic differences among the models and represented the extent of disagreement of the relative magnitude of C fluxes among models. The results showed that the uncertainty in the spatial patterns of NPP followed the magnitude of the mean NPP for both literature-based ($r^2 = 0.66$, $p < 0.001$; Figure 11d) and MsTMIP data ($r^2 = 0.64$, $p < 0.001$; Figure S4b). On the other hand, the uncertainty in the spatial patterns of NBP showed the opposite pattern, which was negatively correlated to the magnitude of NBP, according to the MsTMIP results ($r^2 = 0.23$, $p < 0.001$; Figure S4d).

3.4. International Comparisons

According to a previous synthesis [Ito, 2011] and the average of individual studies (Table S10), the global NPP and NBP were 56.2 and $1.62 \text{ Pg C yr}^{-1}$, respectively (Figures 12a and 12b). Therefore, China accounted for about 6% and 10% of the global NPP and NBP, respectively, based on the literature results. The total NPP in China was equivalent to that of the U.S. and Europe (Table S11) but was smaller than that of Africa [Williams *et al.*, 2007; Ciais *et al.*, 2011]. The total NBP of China was similar to that of Africa and Europe but was lower than that of the U.S. (Figure 12b). The mean NPP of the above regions was comparable to the global average (Figure 12c). The mean NBP of China and Europe was equivalent to the global level, slightly higher than that of Africa, but much smaller than that of the U.S. (Figure 12d). If the study period was constrained to 1981–2000, the China's annual CO_2 emissions from fossil fuels and annual NBP were $0.70 \text{ Pg C yr}^{-1}$ [Boden *et al.*, 2013] and $0.17 \pm 0.09 \text{ Pg C yr}^{-1}$, respectively. Therefore, China's terrestrial ecosystems offset about $24 \pm 13\%$ of the CO_2 emissions from fossil-fuel combustion by itself, which was comparable to the level of the U.S. (26%) and the global level (28%), larger than the level of Europe (7%), but lower than that of Africa (100%). However, the larger estimate of NBP from MsTMIP ($0.32 \pm 0.35 \text{ Pg C yr}^{-1}$) suggested that the China's terrestrial ecosystems might offset more (46%) of the anthropogenic CO_2 emissions, but this estimate was largely influenced by an extreme value (the output of TRIPLEX-GHG; Figure 8) and therefore is highly uncertain.

4. Discussion

4.1. Uncertainty From Different Methods

Diverse assumptions and approaches among studies may introduce the large uncertainty in the net primary productivity (NPP) and net biome productivity (NBP) of terrestrial ecosystems in China. First of all, different approaches attribute the NBP to different flux components, which cause the differences in the outputs among atmospheric inversion, inventory, and process models. The atmospheric inversion models usually overestimate the regional NBP because non- CO_2 emissions (e.g., CO , CH_4 , and volatile organic compounds) from ecosystems were included, whereas the inventory methods could underestimate NBP because they excluded wood and food products [Piao *et al.*, 2009a; Hayes *et al.*, 2012]. The NEP outputs of process models (i.e., NBP without the fire flux, latent, and non- CO_2 fluxes) should theoretically be larger than those from the inventory estimates, which was also revealed by King *et al.* [2012] in North America. However, our literature-based results showed that the process models without nitrogen (N) addition estimated a lower NEP ($0.069 \pm 0.049 \text{ Pg C yr}^{-1}$, the NBP may have been lower if the fire, latent, and non- CO_2 fluxes were added) than those with N addition effect ($0.21 \pm 0.042 \text{ Pg C yr}^{-1}$, $t_{1.84} = 4.00$, $p = 0.065$; Figures 6 and 7) and the inventory methods ($0.17 \pm 0.014 \text{ Pg C yr}^{-1}$, $t_{6.60} = 4.82$, $p = 0.0023$). Considering that all the process models included CO_2 fertilization, the underestimations in NEP might be due to the missing of N addition effect. The MsTMIP results showed that the net C flux (i.e., NBP) values derived from the model simulations with constant N deposition rate ($0.058 \pm 0.011 \text{ Pg C yr}^{-1}$) were lower than those having considered the time-varying N deposition ($0.20 \pm 0.014 \text{ Pg C yr}^{-1}$, $t_{11.85} = 3.35$, $p = 0.0059$) (Figure 8). However, this result reflected two aspects of modeling the N addition effects: (1) the inclusion of C-N coupling and (2) the use of time-varying N deposition data. The inclusion of C-N coupling alone generally decreased estimations of C uptake (0.13 versus $0.37 \text{ Pg C yr}^{-1}$, $t_{2.24} = 6.31$, $p = 0.064$) due to N limitations on CO_2 fertilization [Zaehle and Dalmonech, 2011]. While the inclusion of time-varying N deposition largely reduced this difference because of N fertilization effects. The net result, however, is an estimate of net C uptake for models with C-N coupling ($0.25 \text{ Pg C yr}^{-1}$, $t_{8.42} = 0.99$, $p = 0.35$, compared $0.37 \text{ Pg C yr}^{-1}$ for C-only models). Note that TRIPLEX was excluded from this analysis due to its outlier behavior. These results were consistent with previous findings that the inclusion of N cycle and associated N fertilization generally reduced the estimated NEP at the global scale [Fisher *et al.*, 2014]. Nevertheless, the N control on C fluxes is largely neglected in China because only two models from literature considered the N addition effect.

Even within the same approach, large uncertainty also appeared. For example, the statistical models (e.g., the Miami and Thornthwaite Memorial models) assume that NPP is only related to climatic conditions such as temperature, precipitation, and/or evapotranspiration, being considered as potential NPP [Sun and Zhu, 2000; Zhu *et al.*, 2007a], producing larger estimations than other methods in the literature data set (Figures 1 and 2). In addition, the estimated NPP from light use efficiency (LUE) models was about 1 Pg C yr^{-1} higher

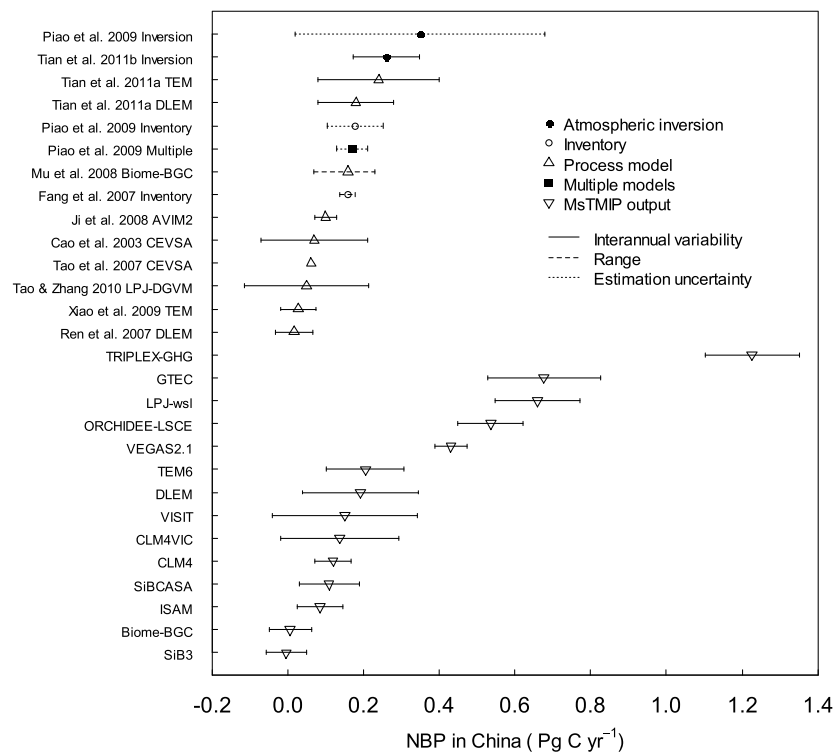


Figure 6. Total net biome productivity (NBP) of China. Interannual variability, standard deviation of annual NBP during the study period; range, difference between the maximum and minimum annual NBP; estimation uncertainty is derived from the difference in model parameters. The references in the y axis can be found in the supporting information.

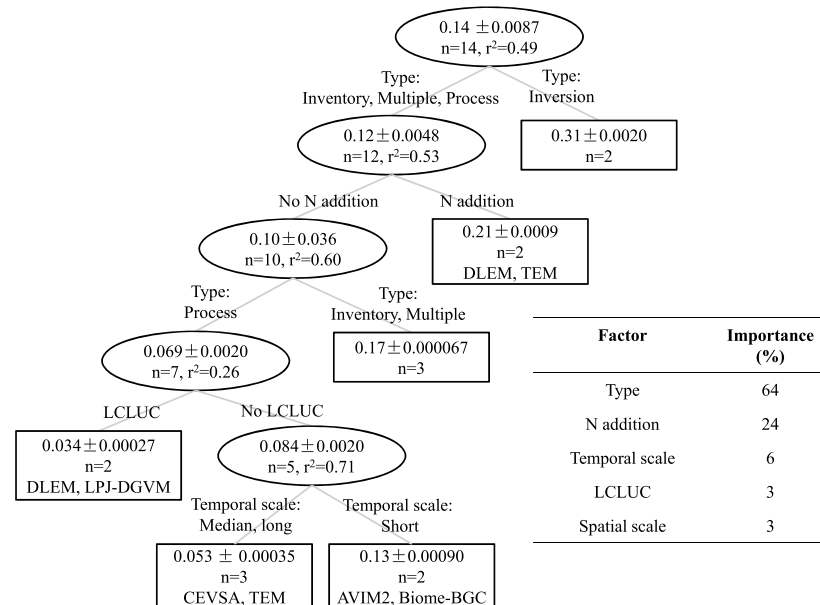


Figure 7. The classification and regression tree (CART) results based on the NBP values from literature. The values in each node are the estimated mean \pm standard deviation (Pg C yr^{-1}). n , the sample size of tree node; r^2 , the explained proportion of variance of a node by the sequent split.

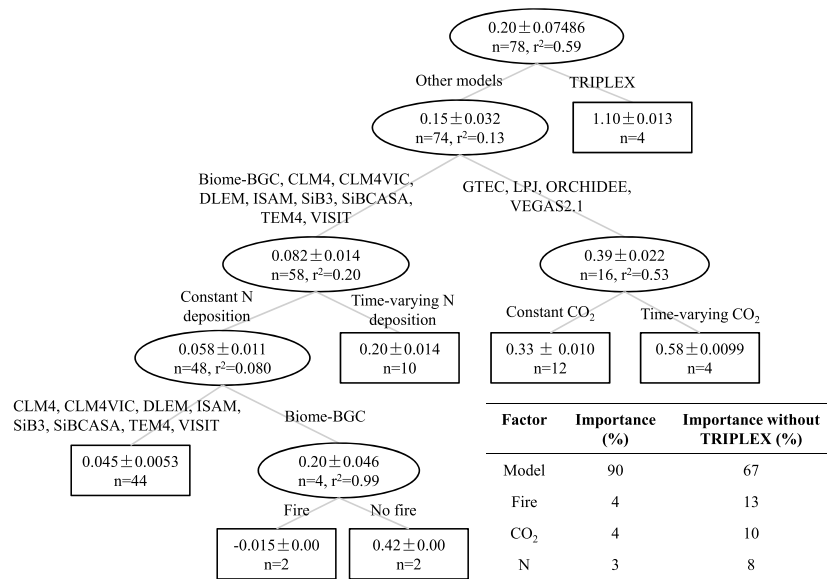


Figure 8. The classification and regression tree (CART) results based on the NBP values from the M_sTMIP data set. The values in each node are the estimated mean \pm standard deviation (Pg C yr^{-1}), n , the sample size of tree node; r^2 , the explained proportion of variance of a node by the sequent split. The relative importance of different factors to overall uncertainty without TRIPLEX outputs was also presented, in order to explore the influence of this model on the results.

than that from enzyme kinetics (EK) models (Figure 2). However, whether the difference resulted from the lack of N fertilization in EK model and/or the high maximum light use efficiency (ϵ_{\max}) in LUE models was not clear. According to the literature-based results, the NPP estimates by models with coarser spatiotemporal scales were larger than those of the models with finer scales (Figure 2), although there was not significantly linear relationships of estimated fluxes against the spatiotemporal scales (Figures S2 and S3). The scale effects found in the CART result might stem from the biases arising from the mixture of heterogeneous land cover and climatic variables encountered when scaling from fine to coarse scales, which caused similar patterns of NPP in other areas [Pierce and Running, 1995; Turner *et al.*, 2000]. These results may have large uncertainty due to small sample size. To better understand the effects of the spatiotemporal scales, it is necessary to have well-designed modeling experiments that only treat spatiotemporal scales as the varying factors.

Overlooking some internal processes or external constraints might also influence the outputs of different models. For example, in literature data set, the inclusion of the N cycle resulted in a much lower NPP (1.58 versus 3.1 Pg C yr^{-1}) due to the effect of N limitation on C uptake (Figure 2) [Fisher *et al.*, 2014]. The models with heterogeneous land cover had higher NPP ($1.12 \text{ Pg C yr}^{-1}$) than those with spatially uniform vegetation, probably because the early versions of LUE models only considered the regulations of climate on LUE and set the ϵ_{\max} too low in highly productive biomes. Globally, the ϵ_{\max} values ranged from 0.09 to 3.5 g C MJ^{-1} whereas the values were 0.389 – $1.259 \text{ g C MJ}^{-1}$ in China (Table S13) [Zhu *et al.*, 2007a]. This large range of ϵ_{\max} probably contributed to the uncertainty of NPP among the LUE models.

In addition, the large uncertainty might be due to a few extreme values. For example, according to the literature data set, the great uncertainty among the statistical models was mainly introduced by an extreme value of $7.44 \text{ Pg C yr}^{-1}$ in 1990 (Figure 1) [Chen *et al.*, 2001] and partly by the interpolation of climate data (300 versus 600 weather stations in Chen *et al.* [2001] and other studies, respectively). Within the LUE models, Global Production Efficiency Model (GloPEM) introduced the largest uncertainty, as it had two extremely large values (Figure 1), which might have arisen from the biased driving data from remote sensing [Dan *et al.*, 2007]. When the driving climate data were corrected further, the GloPEM's output was close to the average of these models [Dan *et al.*, 2015]. For the NBP from the M_sTMIP data, the majority of the overall uncertainty was caused by the dramatic difference between TRIPLEX-GHG and other models (1.10 versus $0.15 \text{ Pg C yr}^{-1}$; Figure 8), which mainly came from the much lower heterotrophic respiration (Rh) in TRIPLEX-GHG (1.83 versus $3.07 \text{ Pg C yr}^{-1}$). However, further studies are needed to understand what caused the higher NBP in TRIPLEX-GHG (e.g., the specialization in wetlands; part of the Rh could be used for CH_4 production [Fisher *et al.*, 2014]).

4.2. Uncertainty From Global Change Factors

According to the MsTMIP results, the importance of model structures outweighed the effects of global change factors on the overall uncertainty (Figures 3 and 8). However, global change factors do affect the outputs of each model and surely determine the regional NPP and NBP to some extent (Figure 4). For example, the effects of N addition were equivalent to 10%–100% of NBP globally [Bala *et al.*, 2013], with a value of $0.079 \pm 0.044 \text{ Pg C yr}^{-1}$ for China's NBP according to the combined data sets of literature and MsTMIP outputs (Figure 4). The uncertainty in the estimated N-induced effects might result from the difference in N application rates and the inconsistency of C–N coupling mechanisms among the models [Tian *et al.*, 2011a; Bala *et al.*, 2013]. Comparisons between the results from field experiments and model outputs may provide some insights to improve the model performance. For example, although the additional N in Dynamic Land Ecosystem Model (DLEM) can alter biomass allocation among organs, the contribution of maintenance respiration to ecosystem respiration, and the decomposition rate of the detritus pool [Tian *et al.*, 2011a; Lu *et al.*, 2012], the positive response of Rh to N addition in the DLEM was opposite to the experimental results with an N-induced decrease in Rh [Janssens *et al.*, 2010; Lu *et al.*, 2011; Zhou *et al.*, 2014]. The potential mechanisms involved might be missed in the DLEM, such as the effects of N addition on soil microbial biomass and activity, interactions between N addition and other global change factors, and complex nonlinear responses, which are limited by our understanding of the mechanisms and the available data.

Climate change and CO₂ fertilization were widely considered to be the drivers of global and regional C flux dynamics [Schimel *et al.*, 2015]. At the global scale, warming increased NPP while increased precipitation and atmospheric CO₂ concentration enhanced both NPP and NBP [Cao *et al.*, 2005; Piao *et al.*, 2009a]. In China, variations in temperature and precipitation increased NPP by $0.11 \pm 0.097 \text{ Pg C yr}^{-1}$, but they seemed to offset each other and resulted in little effect on NBP ($0.020 \pm 0.11 \text{ Pg C yr}^{-1}$; Figure 4). The effect of CO₂ fertilization (0.33 ± 0.19 and $0.12 \pm 0.091 \text{ Pg C yr}^{-1}$ for NPP and NBP, respectively) was more important than the effects of climate change. Since different studies used similar or identical CO₂ observation data, the uncertainty in CO₂ fertilization might be mainly from the forms of the response functions of NPP to rising CO₂ concentration, which were more diverse than the responses to temperature and water conditions [Adams *et al.*, 2004]. Experimental studies exploring the effects of elevated temperature and CO₂ on ecosystem C cycling showed that the short-term responses of ecosystems were quite different from the long-term ones, suggesting that ecosystems may acclimate to the changing climate [Leuzinger and Hättenschwiler, 2013; Bouskill *et al.*, 2014]. How to incorporate this acclimation found in the experiments into mathematical equations in mechanistic models might be a great challenge [Smith and Dukes, 2013].

Land cover and land use change (LCLUC)-induced C emissions were about $1.14 \pm 0.50 \text{ Pg C}$ at the global scale [Houghton *et al.*, 2012]. However, in China, LCLUC might enhance the NPP and NBP through afforestation and tree growth and reduce them by sudden changes in land use or degradation of natural ecosystems, resulting in a neutral effect with large uncertainty (-0.0075 ± 0.19 and $0.0088 \pm 0.069 \text{ Pg C yr}^{-1}$ for NPP and NBP, respectively; Figure 4). This uncertainty might largely result from the inconsistency in land cover change among the studies. For example, Ge *et al.* [2008] and Liu and Tian [2010] showed that the forest area increased and the cropland area decreased, although Liu *et al.* [2005] suggested an increasing trend for cropland during 1990–2000. Despite the importance of wetlands and human settlements, changes in these areas have not been considered in the models, which may introduce additional uncertainty in the future [Ito *et al.*, 2008; Houghton *et al.*, 2012].

The effects of O₃ and fire on China's NPP and NBP were the least studied. The negative effects of O₃ on stomatal conductance and photosynthesis [Lombardozzi *et al.*, 2013] seemed negligible at the regional scale according to our comparative study (Figure 4b) [Ren *et al.*, 2007; Tian *et al.*, 2011a]. However, the uncertainty and its potential sources caused by increased O₃ in China are difficult to explore because only a few studies had been conducted and our understanding about this factor is poor. The fire flux is considered to be the difference between NEP and NBP when latent fluxes and non-CO₂ fluxes are negligible and has been estimated to decrease global NBP by $1\text{--}2 \text{ Pg C yr}^{-1}$ [Li *et al.*, 2014] and China's NBP by $0.17 \pm 0.15 \text{ Pg C yr}^{-1}$ in the process models (Figure 4b). However, this flux might be overestimated in China. Overall, the prognostic models (i.e., Biome-BGC, CLM4, CLM4VIC, and LPJ-DGVM), which set prescribed fire rates for each plant functional type and were not constrained by burned areas data, had much larger estimates ($0.22 \pm 0.14 \text{ Pg C yr}^{-1}$)

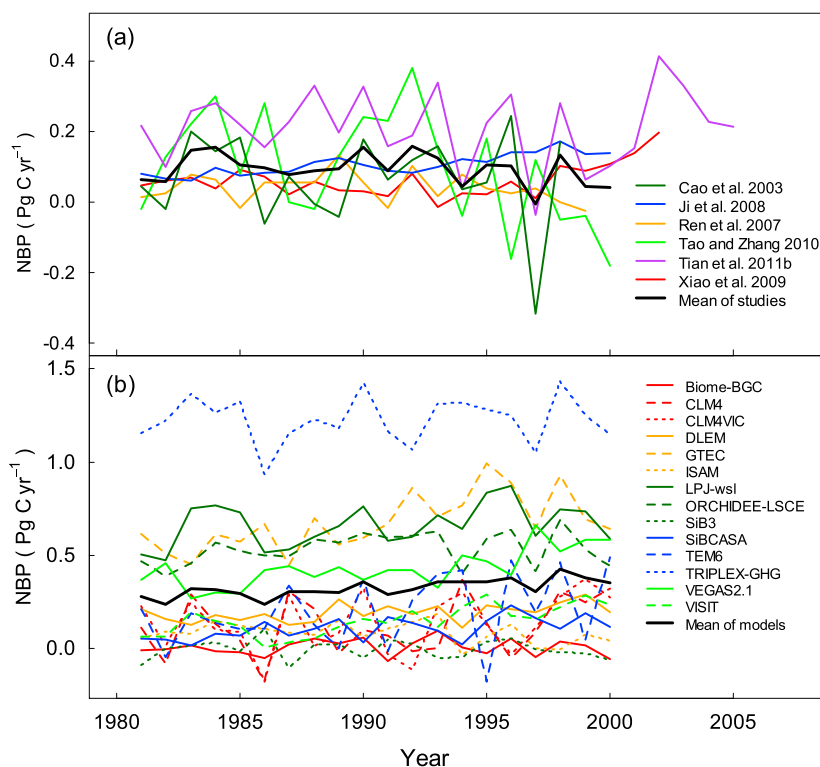


Figure 9. Time series of China's NBP from the (a) literature (1981–2005) and (b) MsTMIP (1981–2000) data sets. The references in the legend can be found in the supporting information.

than those based on burned areas data ($0.030 \pm 0.037 \text{ Pg C yr}^{-1}$, $t_{4,94} = 2.87$, $p = 0.036$, TEM6 and DLEM). Other methods that mainly aimed to estimate fire flux in China gave even lower values. For example, a recent estimate based on Global Fire Emissions Database was $0.021 \text{ Pg C yr}^{-1}$ during 2001–2010 (Carbon Tracker, <http://www.carbontracker.net/fluxmaps.php>). Combining inventory, remote sensing, and terrestrial ecosystem modeling gave an estimate of $0.011 \text{ Pg C yr}^{-1}$ during 1950–2000 [Lü et al., 2006]. Another study based on inventory data suggested that the fire emission from 1991 to 2000 was $0.0074\text{--}0.010 \text{ Pg C yr}^{-1}$ [Tian et al., 2003]. The small fire flux was largely because China's government adopted a policy of suppressing wildfire as intensively as possible during the study period [Tian et al., 2003].

4.3. Uncertainty of Temporal and Spatial Patterns

Besides the changes in mean annual values among models, the IAV in China's NPP and NBP also exhibited large uncertainty. During 1981–2000, the IAV in China's NPP and NBP was $0.026\text{--}0.28$, and $0.029\text{--}0.19 \text{ Pg C yr}^{-1}$, respectively (Figures 5 and 9). For NPP, different studies presented a consistent interannual pattern (Figure 5) and a significantly increasing rate of 0.012 Pg since 1981 based on both literature-based and MsTMIP data (0.38% , $r^2 = 0.47$, $p < 0.001$). At the global scale, the fluctuations in annual NPP are related to the climatic variations, natural disturbances, human activities, and vegetation dynamics [Bastos et al., 2013; Piao et al., 2013], among which the effects of CO_2 and precipitation are mostly highlighted [Piao et al., 2009b]. In China, annual NPP was also correlated with annual temperature [Fang et al., 2003; Piao et al., 2005; Mao et al., 2010], annual precipitation [Piao et al., 2001; Cao et al., 2003; Tao et al., 2003; Liang and Xie, 2006; Mu et al., 2008], and large-scale climatic events [Zhu et al., 2007b]. Among these factors, precipitation seemed to be the most important (explaining 33% and 44% of variance in annual NPP from the literature-based and MsTMIP results, respectively), followed by CO_2 (27% and 19%), temperature (17% and 22%), and radiation (2% for both). However, the contribution of other global change factors, such as O_3 concentrations, N addition, and LCLUC, to the temporal variations in China's NPP is not clear, although their effects might depend on the sensitivity of C cycling to these factors.

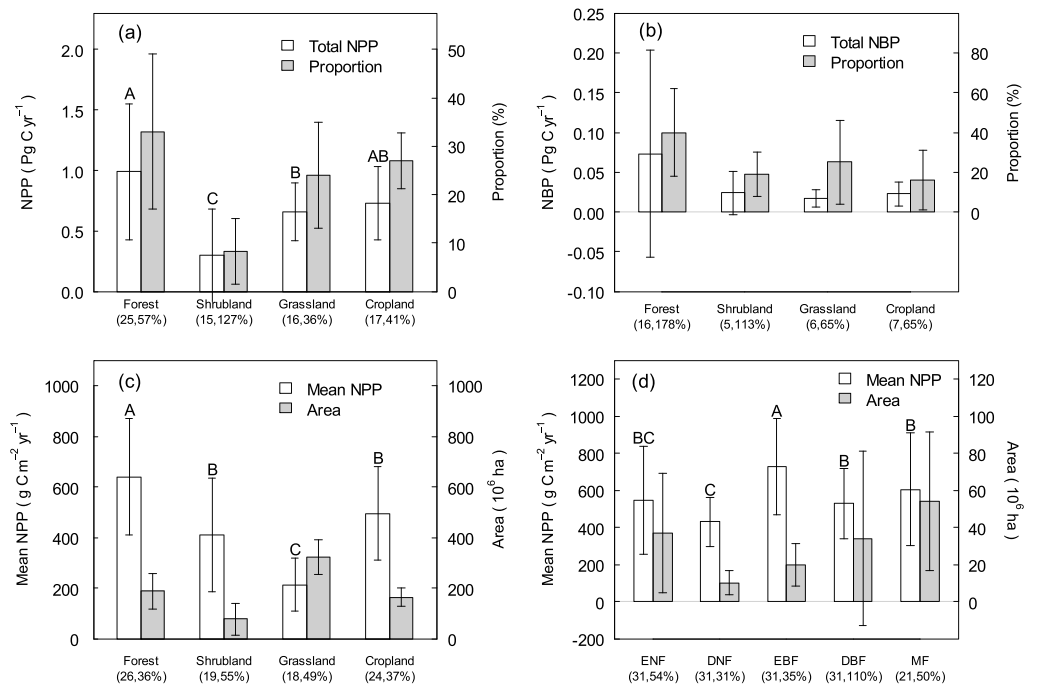


Figure 10. (a) Different biomes' NPP and their proportion to total NPP, (b) different biomes' NBP and their contribution to total NBP, (c) mean NPP and area of main biomes, and (d) forest types. The Kruskal-Wallis test was used for multiple comparisons ($\alpha = 0.05$). The error bars represented the SDs.

Conversely, the interannual patterns of China's NBP were not consistent among studies (Figure 9). Therefore, the trend of NBP [Xiao *et al.*, 2009; Tao and Zhang, 2010; Tian *et al.*, 2011b] and the correlations between NBP and climatic variations [Cao *et al.*, 2003; Mu *et al.*, 2008; Xiao *et al.*, 2009] found in previous studies were less reliable than those of NPP. As most models did not have a fire module, these results suggested that the Rh introduced additional uncertainty into the NEP and thus NBP due to our limited understanding of the underlying processes involved in Rh. Reproducing a consistent interannual pattern in NEP is also very difficult at the ecosystem scale [Keenan *et al.*, 2012], which might largely be due to the changing responses of C cycling to climatic variations from year to year [Hui *et al.*, 2003; Richardson *et al.*, 2007; Shao *et al.*, 2015]. Progresses in simulating the functional change at the ecosystem level and scaling it up to the regional and global scales could largely enhance the reliability of model predictions in future global climate change scenarios.

The uncertainty in the total NPP and NBP of a certain biome was derived from both the mean value and the covering area (Figure 10). All these estimations had large uncertainty, especially for forests and shrublands. The discrepancy in mean NPP and NBP among models mainly arose from the estimation methods, while the difference of biome area was due to the discrepancies in vegetation classification criteria [De Cáceres and Wiser, 2012], the difficulty of classifying the transient biomes (e.g., shrubland) and the LCLUC. Spatially, NPP exhibited high heterogeneity, and the discrepancy in spatial patterns among studies was more obvious in the southern and eastern China (Figure 11d). This was partly due to the complicated topography and the diverse vegetation in these areas, which had both low and highly productive biomes from grassland to evergreen broadleaf forest. Interestingly, although the spatial patterns of NBP and NPP were similar, the most uncertain NBP was seen in low productivity areas (Figures S4c and S4d). This suggested that the differences of NPP among the models were diminished in highly productive areas but were amplified in less productive ones. Moreover, the lack of local adaptation and acclimation to climate change might constrain a model's ability to reproduce the spatial patterns of C fluxes reliably, because the response mechanisms of ecosystems to climatic variations might be very different even for the same biome but distributed in different regions [Yuan *et al.*, 2011; Niu *et al.*, 2012].

In the global context, China contributed significantly to the global productivity (6%; Figure 12a) and the global C sink (10%; Figure 12b). The area-averaged productivity and C sink and the ability of China to offset the

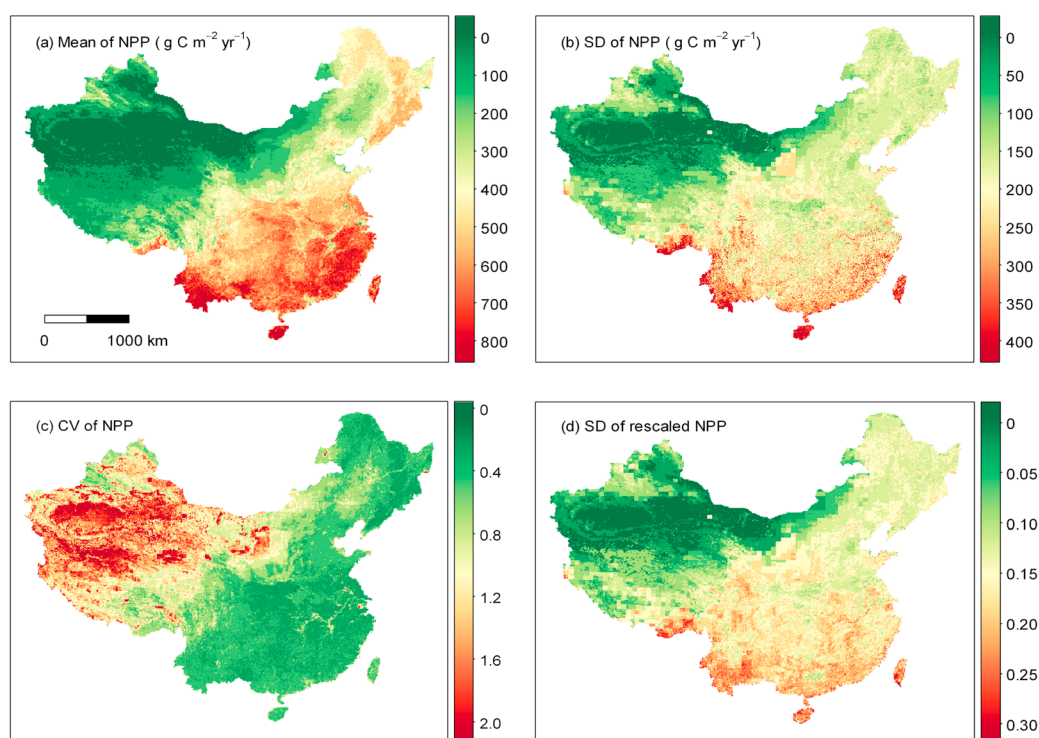


Figure 11. The spatial patterns of the (a) mean, (b) standard deviation (SD), and (c) coefficient of variation (CV) of NPP, and the (d) SD of the rescaled NPP among 16 models from the literature. The spatial NPP data were taken from Sun and Zhu [2000], He et al. [2005], Meng et al. [2005], Dan et al. [2007] (six estimations), Zhu et al. [2007a], Gao and Liu [2008] (five estimations), and Tao and Zhang [2010]. In Figure 11d, the rescaled NPP was calculated as $(x - \min(x)) / \text{range}(x)$, where x is the NPP in a certain NPP map, and the standard deviation of the rescaled NPP at a certain pixel among 16 maps was then calculated.

CO₂ emissions from industry (24%) during 1981–2000 were close to the global averages. Recent estimations showed that China accounted for 28% of global CO₂ emissions in 2013 [Le Quéré et al., 2014]. On the other hand, Yu et al. [2014] suggested that the East Asian monsoon subtropical forests, a large proportion of which is located in China, were more efficient than Asian tropical and temperate forests in the terms of being a C sink. Therefore, further research should be carried out to determine how the China's terrestrial ecosystems can or will mitigate global warming, which is important for international negotiations. However, the estimated global NPP and NBP and those of other regions also had great uncertainty, which should be reduced before conducting a reliable comparison.

4.4. Implications for C Cycle Models and Future Experiments

Despite great progress over the recent decades, the uncertainty in the estimated land C sink has not yet been reduced since Intergovernmental Panel on Climate Change AR3 (Third Assessment Report) [Ciais et al., 2013]. The difficulty may be largely derived from the insufficient understanding on the underlying mechanisms of C cycling and its spatiotemporal dynamics. Therefore, extensive efforts should be made to improve predictions of the terrestrial C sink under climate change. Our results from the synthesis of the published NPP and NBP data may provide some insights into how to reduce the uncertainty through the development and improvement of land surface models as well as into the design of manipulative experiments in the future. First, large uncertainty occurred among studies using diverse methods, suggesting that model comparisons (e.g., MsTMIP [Huntzinger et al., 2013; Mao et al., 2015; Schwalm et al., 2015]) and benchmarking procedure such as the Climate Model Intercomparison Project, International Land Model Benchmarking Project, Trends in Net Land-Atmosphere Carbon Exchange, and Inter-Sectoral Impact Model Intercomparison Project [Luo et al., 2012; Todd-Brown et al., 2013; Fisher et al., 2014; Yan et al., 2014] are necessary to identify the pros and cons of different methods. Meanwhile, manipulative

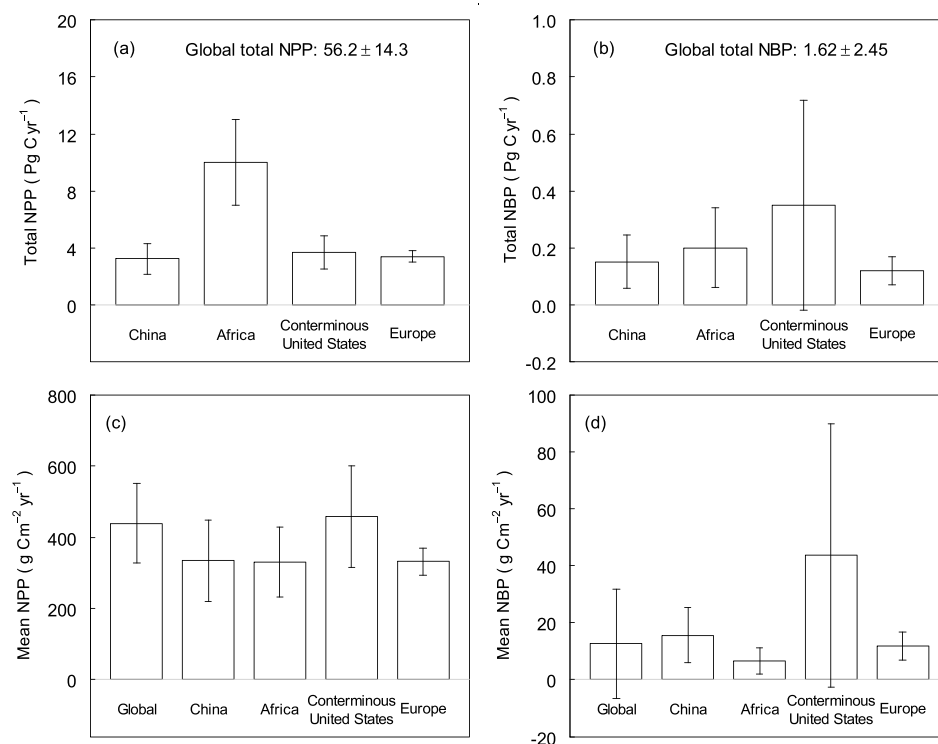


Figure 12. The international comparison of (a and b) total and (c and d) area averaged mean, global and regional NPP (Figures 12a and 12c) and NBP (Figures 12b and 12d). Global NPP was taken from Ito [2011], global NBP was taken from 75 estimations (Table S10), and Africa's NPP and NBP were from Williams *et al.* [2007] and Ciais *et al.* [2011], respectively. The conterminous United States' NPP and NBP were from 5 and 10 estimations, respectively (Table S11). The Europe's NPP and NBP were from eight and four estimations (Table S11), respectively. The error bars represented the SDs.

experiments may need to coordinate with process studies and modeling synthesis to evaluate the underlying mechanisms and develop generalizable knowledge across scales to validate model performance and prediction [Luo *et al.*, 2011; Fraser *et al.*, 2013].

Second, the available data are usually insufficient to identify the alternative model structures and constrain the parameters compared to the large number of parameters in current models. Therefore, the observations and experiments should be carried out in more representative and efficient ways for land surface modeling. Our study showed asymmetric uncertainty among biomes in China, with forests and shrublands having greater uncertainty, suggesting that more attention should be focused in these two biomes. Studies on wetlands, tropical rain forests, tundra, and ecosystems in permafrost areas are also needed because of their important roles in the C cycle and relatively little attention paid so far [Elmendorf *et al.*, 2012; Zhou *et al.*, 2013; Sjögersten *et al.*, 2014; Schuur *et al.*, 2015]. Moreover, previous studies have suggested that flux- and biometric-based data are complementary for constraining model parameters [Du *et al.*, 2015], indicating that data should be collected for different aspects of C cycling.

Third, in order to predict the global C balance in the future, the models are supposed to reproduce the spatiotemporal patterns of ecosystem C cycling, which largely challenges modelers. We found that the models provided quite diverse interannual patterns of NBP in China, being consistent with a previous study, which generally failed to reproduce the observed IAV of NEP at the ecosystem scale [Keenan *et al.*, 2012]. Spatially, the model performance might not be the same among different biomes or regions. For example, many models were highly biased in the tropics due to the lack of phosphorus limitation on productivity [Bonan *et al.*, 2011]. Calibrating and validating models in diverse regions might help to improve the model performance across space and time. However, evaluating the model behavior temporally and spatially is of great importance for reducing model uncertainty and providing accurate results.

Acknowledgments

The data used in this analysis are shown in the supporting information. We thank the three anonymous reviewers for their constructive comments and suggestions. This research was financially supported by the National Natural Science Foundation of China (Grant 31370489), the Program for Professor of Special Appointment (Eastern Scholar) at the Shanghai Institutions of Higher Learning, and the national "Thousand Young Talents" Program in China. Funding for the Multi-scale synthesis and Terrestrial Model Intercomparison Project (MstMIP; <http://nacp.ornl.gov/MstMIP.shtm>) activity was provided through NASA ROSES Grant NNX10AG01A. Data management support for preparing, documenting, and distributing model driver and output data was performed by the Modeling and Synthesis Thematic Data Center at Oak Ridge National Laboratory (ORNL; <http://nacp.ornl.gov>), with funding through NASA ROSES Grant NNH10AN681. Finalized MstMIP data products are archived at the ORNL DAAC (<http://daac.ornl.gov>). This is MstMIP contribution #5. Acknowledgments for specific MstMIP participating models: Biome-BGC: Biome-BGC code was provided by the Numerical Terradynamic Simulation Group at the University of Montana. The computational facilities provided by NASA Earth Exchange at NASA Ames Research Center. CLM: This research is supported in part by the U.S. Department of Energy (DOE), Office of Science, Biological, and Environmental Research. Oak Ridge National Laboratory is managed by UTBATTLE for DOE under contract DE-AC05-00OR22725. CLM4VIC: CLM4VIC simulations were supported in part by the U.S. Department of Energy (DOE), Office of Science, Biological, and Environmental Research (BER) through the Earth System Modeling program and performed using the Environmental Molecular Sciences Laboratory, a national scientific user facility sponsored by the U.S. DOE-BER and located at Pacific Northwest National Laboratory (PNNL). Participation of M. Huang in the MstMIP synthesis is supported by the U.S. DOE-BER through the Subsurface Biogeochemical Research Program (SBR) as part of the SBR Scientific Focus Area (SFA) at the Pacific Northwest National Laboratory (PNNL). PNNL is operated for the U.S. DOE by BATTELLE Memorial Institute under contract DE-AC05-76RLO1830. DLEM: The Dynamic Land Ecosystem Model (DLEM) developed in the International Center for Climate and Global Change Research at Auburn University has been supported by NASA Interdisciplinary Science Program, NASA Land Cover/Land Use Change Program (LCLUC), NASA Terrestrial Ecology Program, NASA Atmospheric Composition Modeling and Analysis Program; NSF Dynamics of

References

- Adams, B., A. White, and T. M. Lenton (2004), An analysis of some diverse approaches to modeling terrestrial net primary productivity, *Ecol. Model.*, **177**, 353–391, doi:10.1016/j.ecolmodel.2004.03.014.
- Bala, G., N. Devaraju, R. K. Chaturvedi, and R. Nemani (2013), Nitrogen deposition: How important is it for global terrestrial carbon uptake?, *Biogeosciences*, **10**, 7147–7160, doi:10.5194/bg-10-7147-2013.
- Baldocchi, D. (2008), 'Breathing' of the terrestrial biosphere: Lessons learned from a global network of carbon dioxide flux measurement systems, *Aust. J. Bot.*, **56**, 1–26, doi:10.1071/BT07151.
- Bastos, A., S. W. Running, C. Gouveia, and R. M. Trigo (2013), The global NPP dependence on ENSO: La Niña and the extraordinary year of 2011, *J. Geophys. Res.*, **B**, **118**, 1247–1255, doi:10.1002/jgrg.20100.
- Bi, J., and J. Chung (2011), Identification of drivers of overall liking-determination of relative importances of regressor variables, *J. Sens. Stud.*, **26**, 245–254, doi:10.1111/j.1745-459X.2011.00340.x.
- Boden, T. A., G. Marland, and R. J. Andres (2013), *Global, Regional, and National Fossil-fuel CO₂ Emissions*, Carbon Dioxide Information Analysis Center, Oak Ridge National Laboratory, U.S. Department of Energy, Oak Ridge, Tenn., doi:10.3334/CDIAC/00001_V2013.
- Bonan, C. B., P. J. Lawrence, K. W. Oleson, S. Levis, M. Jung, M. Reichstein, D. M. Lawrence, and S. C. Swenson (2011), Improving canopy processes in the community land model version 4 (CLM4) using global flux fields empirically inferred from FLUXNET data, *J. Geophys. Res.*, **116**, G02014, doi:10.1029/2010JG001593.
- Bouskill, N. J., W. J. Riley, and J. Y. Tang (2014), Meta-analysis of high-latitude nitrogen-addition and warming studies implies ecological mechanisms overlooked by land models, *Biogeosciences*, **11**, 6969–6983, doi:10.5194/bg-11-6969-2014.
- Breiman, L., J. H. Friedman, R. A. Olshen, and C. J. Stone (1984), *Classification and Regression Trees*, Wadsworth, Belmont, Calif.
- Canadell, J. G., C. Le Quéré, M. R. Raupach, C. B. Field, E. T. Buitenhuis, P. Ciais, T. J. Conway, N. P. Gillett, R. A. Houghton, and G. Marland (2007a), Contributions to accelerating atmospheric CO₂ growth from economic activity, carbon intensity, and efficiency of natural sinks, *Proc. Natl. Acad. Sci. U.S.A.*, **104**, 18,866–18,870, doi:10.1073/pnas.0702737104.
- Canadell, J. G., M. U. F. Kirschbaum, W. A. Kurz, M. -J. Sanz, B. Schlamadinger, and Y. Yamagata (2007b), Factoring out natural and indirect human effects on terrestrial carbon sources and sinks, *Environ. Sci. Policy*, **10**, 370–384, doi:10.1016/j.envsci.2007.01.009.
- Cao, M., S. D. Prince, K. Li, B. Tao, J. Small, and X. Shao (2003), Response of terrestrial carbon uptake to climate interannual variability in China, *Global Change Biol.*, **9**, 536–546, doi:10.1046/j.1365-2486.2003.00617.x.
- Cao, M., S. D. Prince, B. Tao, J. Small, and K. Li (2005), Regional pattern and interannual variations in global terrestrial carbon uptake in response to changes in climate and atmospheric CO₂, *Tellus*, **57B**, 210–217, doi:10.1111/j.1600-0889.2005.00146.x.
- Chapin, F. S., et al. (2006), Reconciling carbon-cycle concepts, terminology and methods, *Ecosystems*, **9**, 1041–1050, doi:10.1007/s10021-005-0105-7.
- Chen, H., et al. (2013), Methane emissions from rice paddies natural wetlands, lakes in China: Synthesis new estimate, *Global Change Biol.*, **19**, 19–32, doi:10.1111/gcb.12034.
- Chen, L., G. Liu, and X. Feng (2001), Estimation of net primary productivity of terrestrial vegetation in China by remote sensing, *Acta Bot. Sin.*, **43**, 1191–1198.
- Ciais, P., A. Bombelli, M. Williams, S. L. Piao, J. Chave, C. M. Ryan, M. Henry, P. Brender, and R. Valentini (2011), The carbon balance of Africa: Synthesis of recent research studies, *Phil. Trans. R. Soc. A*, **369**, 2038–2057, doi:10.1098/rsta.2010.0328.
- Ciais, P., et al. (2013), Carbon and other biogeochemical cycles, in *Climate Change 2013: The Physical Science Basis*, edited by T. F. Stocker et al., pp. 465–570, Cambridge Univ. Press, Cambridge, U. K., and New York.
- Cramer, W., D. W. Kicklighter, A. Bondeau, B. Moore, G. Churkina, B. Nemry, A. Ruimy, A. L. Schloss, and The Participants of the Potsdam NPP Model Intercomparison (1999), Comparing global models of terrestrial net primary productivity (NPP): Overview and key results, *Global Change Biol.*, **5**, 1–15, doi:10.1046/j.1365-2486.1999.00009.x.
- Dan, L., J. Ji, and Y. He (2007), Use of ISLSCP II data to intercompare and validate the terrestrial net primary production in a land surface model coupled to a general circulation model, *J. Geophys. Res.*, **112**, D02590, doi:10.1029/2006JD007721.
- Dan, L., F. Cao, and R. Cao (2015), The improvement of a regional climate model by coupling a land surface model with eco-physiological processes: A case study in 1998, *Clim. Change*, **129**, 457–470, doi:10.1007/s10584-013-0997-8.
- De'ath, G., and K. E. Fabricius (2000), Classification and regression trees: A powerful yet simple technique for ecological data analysis, *Ecology*, **81**, 3178–3192, doi:10.1890/0012-9658(2000)081[3178:CARTAP]2.0.CO;2.
- De Cáceres, M., and S. K. Wiser (2012), Towards consistency in vegetation classification, *J. Veg. Sci.*, **23**, 387–393, doi:10.1111/j.1654-1103.2011.01354.x.
- Deng, X., J. Han, J. Zhan, and Y. Zhao (2009), Management strategies and their evaluation for carbon sequestration in cropland, *Agric. Sci. Technol.*, **10**, 134–139.
- Du, Z., Y. Nie, Y. He, G. Yu, H. Wang, and X. Zhou (2015), Complementarity of flux- and biometric-based data to constrain parameters in a terrestrial carbon model, *Tellus B*, **67**, doi:10.3402/tellusb.v67.24102.
- Elmendorf, S. C., et al. (2012), Global assessment of experimental climate warming on tundra vegetation: heterogeneity over space and time, *Ecol. Lett.*, **15**, 164–175, doi:10.1111/j.1461-0248.2011.01716.x.
- Fang, J., S. Piao, C. B. Field, Y. Pan, Q. Guo, L. Zhou, C. Peng, and S. Tao (2003), Increasing net primary production in China from 1982 to 1999, *Front. Ecol. Environ.*, **1**, 293–297, doi:10.1890/1540-9295(2003)001[0294:INPPIC]2.0.CO;2.
- Fisher, J. B., D. N. Huntzinger, C. R. Schwalm, and S. Sitch (2014), Modeling the terrestrial biosphere, *Annu. Rev. Environ. Resour.*, **39**, 91–123, doi:10.1146/annurev-environ-012913-093456.
- Fraser, L. H., et al. (2013), Coordinated distributed experiments: An emerging tool for testing global hypotheses in ecology and environmental science, *Front. Ecol. Environ.*, **11**, 147–155, doi:10.1890/110279.
- Friedlingstein, P., P. Cox, and R. Betts (2006), Climate-carbon cycle feedback analysis: results from the C⁴MIP Model Intercomparison, *J. Clim.*, **19**, 3337–3353, doi:10.1175/JCLI3800.1.
- Gao, Z., and J. Liu (2008), Simulation study of China's net primary production, *Chinese Sci. Bull.*, **53**, 434–443, doi:10.1007/s11434-008-0097-8.
- Ge, Q., J. Dai, F. He, Y. Pan, and M. Wang (2008), Land use changes and their relations with carbon cycles over the past 300 a in China, *Sci. China Ser. D*, **51**, 871–884, doi:10.1007/s11430-008-0046-z.
- Gravetter, F. J., and L. B. Wallnau (2007), *Statistics for the Behavioral Sciences*, Delmar Publishers, New York.
- Gregg, J. S., R. J. Andres, and G. Marland (2008), China: Emissions pattern of the world leader in CO₂ emissions from fossil fuel consumption and cement production, *Geophys. Res. Lett.*, **35**, L08806, doi:10.1029/2007GL032887.
- Gurney, K. R., et al. (2003), TransCom3 CO₂ inversion intercomparison: 1. Annual mean control results and sensitivity to transport and prior flux information, *Tellus B*, **55**, 555–579, doi:10.1034/j.1600-0889.2003.00049.x.

Coupled Natural-Human System Program, Decadal and Regional Climate Prediction using Earth System Models; DOE National Institute for Climate Change Research; USDA AFRI Program; and EPA STAR Program. ISAM: Integrated Science Assessment Model (ISAM) simulations were supported by the U.S. National Science Foundation (NSF-AGS-12-43071 and NSF-EFRI-083598), the USDA National Institute of Food and Agriculture (2011-68002-30220), the U.S. Department of Energy (DOE) Office of Science (DOE-DE-SC0006706), and the NASA Land Cover and Land Use Change Program (NNX14AD94G). ISAM simulations were carried out at the National Energy Research Scientific Computing Center, which is supported by the Office of Science of the U.S. Department of Energy under contract DE-AC02-05CH11231, and at the Blue Waters sustained-petascale computing, University of Illinois at Urbana-Champaign, which is supported by the National Science Foundation (awards OCI-0725070 and ACI-1238993) and the state of Illinois. LPJ-wsl: This work was conducted at LSCE, France, using a modified version of the LPJ version 3.1 model, originally made available by the Potsdam Institute for Climate Impact Research. ORCHIDEE-LSCE: ORCHIDEE is a global land surface model developed at the IPSL institute in France. The simulations were performed with the support of the GhG Europe FP7 grant with computing facilities provided by LSCE (Laboratoire des Sciences du Climat et de l'Environnement) or TGCC (Très Grand Centre de Calcul). TRIPLEX-GHG: TRIPLEX-GHG developed at University of Quebec at Montreal (Canada) and Northwest A&F University (China) has been supported by the National Basic Research Program of China (2013CB956602) and the National Science and Engineering Research Council of Canada (NSERC) Discover Grant. VISIT: VISIT was developed at the National Institute for Environmental Studies, Japan. This work was mostly conducted during a visiting stay at Oak Ridge National Laboratory.

- Hayes, D. J., et al. (2012), Reconciling estimates of the contemporary North American carbon balance among terrestrial biosphere models, atmospheric inversions, and a new approach for estimating net ecosystem exchange from inventory-based data, *Global Change Biol.*, **18**, 1282–1299, doi:10.1111/j.1365-2486.2011.02627.x.
- He, Y., W. Dong, J. Ji, and L. Dan (2005), The net primary production simulation of terrestrial ecosystems in China by AVIM, *Adv. Earth Sci.*, **20**, 345–349, doi:10.11867/j.issn.1001-8166.2005.03.0345.
- Heimann, M., and M. Reichstein (2008), Terrestrial ecosystem carbon dynamics and climate feedbacks, *Nature*, **451**, 289–292, doi:10.1038/nature06591.
- Houghton, R. A., J. I. House, J. Pongratz, G. R. van der Werf, R. S. DeFries, M. C. Hansen, C. Le Quéré, and N. Ramankutty (2012), Carbon emissions from land use and land-cover change, *Biogeosciences*, **9**, 5125–5142, doi:10.5194/bg-9-5125-2012.
- Hui, D., Y. Luo, and G. Katul (2003), Partitioning interannual variability in net ecosystem exchange between climatic variability and functional change, *Tree Physiol.*, **23**, 433–442, doi:10.1093/treephys/23.7.433.
- Huntzinger, D. N., et al. (2012), North American Carbon Project (NACP) regional interim synthesis: Terrestrial biospheric model intercomparison, *Ecol. Model.*, **224**, 144–157, doi:10.1016/j.ecolmodel.2012.02.004.
- Huntzinger, D. N., et al. (2013), The North American Carbon Program Multi-scale Synthesis and Terrestrial Model Intercomparison Project – Part 1: Overview and experimental design, *Geosci. Model Dev.*, **6**, 2121–2133, doi:10.5194/gmd-6-2121-2013.
- Huntzinger, D. N., et al. (2015), NACP MtTIP: Global 0.5-deg terrestrial biosphere model outputs, (version 1) in standard format data set. Available on-line [http://daac.ornl.gov] from Oak Ridge National Laboratory Distributed Active Archive Center, Oak Ridge, Tenn., doi:10.3334/ORNLDAAAC/1225.
- Intergovernmental Panel on Climate Change (2013), *Climate Change 2013: The Physical Science Basis*, Cambridge Univ. Press, Cambridge.
- Ito, A. (2011), A historical meta-analysis of global terrestrial net primary productivity: Are estimates converging?, *Global Change Biol.*, **17**, 3161–3175, doi:10.1111/j.1365-2486.2011.02450.x.
- Ito, A., et al. (2008), Can we reconcile differences in estimates of carbon fluxes from land-use change and forestry for the 1990s?, *Atmos. Chem. Phys.*, **8**, 3291–3310, doi:10.1029/2010JG001314.
- Janssens, I. A., W. Dieleman, and S. Luysaert (2010), Reduction of forest soil respiration in response to nitrogen deposition, *Nat. Geosci.*, **3**, 315–322, doi:10.1038/ngeo844.
- Jung, M., et al. (2007), Uncertainties of modeling gross primary productivity over Europe: A systematic study on the effects of using different drivers and terrestrial biosphere models, *Global Biogeochem. Cycles*, **21**, GB4021, doi:10.1029/2006GB002915.
- Jung, M., et al. (2011), Global patterns of land-atmosphere fluxes of carbon dioxide, latent heat, and sensible heat derived from eddy covariance, satellite, and meteorological observations, *J. Geophys. Res.*, **116**, G00J07, doi:10.1029/2010JG001566.
- Keenan, T. F., et al. (2012), Terrestrial biosphere model performance for inter-annual variability of land-atmosphere CO₂ exchange, *Global Change Biol.*, **18**, 1971–1987, doi:10.1111/j.1365-2486.2012.02678.x.
- King, A. W., D. J. Hayes, D. N. Huntzinger, T. O. West, and W. M. Post (2012), North American carbon dioxide sources and sinks: Magnitude, attribution, and uncertainty, *Front. Ecol. Environ.*, **10**, 512–519, doi:10.1890/120066.
- Le Quéré, C., et al. (2009), Trends in the sources and sinks of carbon dioxide, *Nat. Geosci.*, **2**, 831–836, doi:10.1038/ngeo689.
- Le Quéré, C., et al. (2014), Global carbon budget 2014, *Earth Syst. Sci. Data Discuss.*, **7**, 521–610, doi:10.5194/essdd-7-521-2014.
- Le Quéré, C., et al. (2015), Global carbon budget 2015, *Earth Syst. Sci. Data*, **7**, 349–396, doi:10.5194/essd-7-349-2015.
- Leuzinger, S., and S. Hättenschwiler (2013), Beyond global change: Lessons from 25 years of CO₂ research, *Oecologia*, **171**, 639–651, doi:10.1007/s00442-012-2584-5.
- Li, F., B. Bond-Lamberty, and S. Levis (2014), Quantifying the role of fire in the Earth system - Part 2: Impact on the net carbon balance of global terrestrial ecosystems for the 20th century, *Biogeosciences*, **11**, 1345–1360, doi:10.5194/bg-11-1345-2014.
- Liang, M., and Z. Xie (2006), Simulations of climate effects on vegetation distribution and net primary production in China, *Clim. Environ. Res.*, **11**, 582–592, doi:10.3878/j.issn.1006-9585.2006.05.03.
- Lindeman, R. H., P. F. Merenda, and R. Z. Gold (1980), *Introduction to Bivariate and Multivariate Analysis*, Glenview IL, Foresman.
- Liu, J., M. Liu, H. Tian, D. Zhuang, Z. Zhang, W. Zhang, X. Tang, and X. Deng (2005), Spatial and temporal patterns of China's cropland during 1990–2000: An analysis based on Landsat TM data, *Remote Sens. Environ.*, **98**, 442–456, doi:10.1016/j.rse.2005.08.012.
- Liu, M., and H. Tian (2010), China's land cover and land use change from 1700 to 2005: Estimations from high-resolution satellite data and historical archives, *Global Biogeochem. Cycles*, **24**, GB3003, doi:10.1029/2009GB003687.
- Lombardozzi, D., J. P. Sparks, and G. Bonan (2013), Integrating O₃ influences on terrestrial processes: Photosynthetic and stomatal response data available for regional and global modeling, *Biogeosciences*, **10**, 6815–6831, doi:10.5194/bg-10-6815-2013.
- Lü, A., H. Tian, M. Liu, J. Liu, and J. M. Melillo (2006), Spatial and temporal patterns of carbon emissions from forest fires in China from 1950 to 2000, *J. Geophys. Res.*, **111**, D05313, doi:10.1029/2005JD006198.
- Lu, C., H. Tian, M. Liu, W. Ren, X. Xu, G. Chen, and C. Zhang (2012), Effect of nitrogen deposition on China's terrestrial carbon uptake in the context of multifactor environmental changes, *Ecol. Appl.*, **22**, 53–75, doi:10.1890/10-1685.1.
- Lu, M., X. Zhou, Y. Luo, Y. Yang, C. Fang, J. Chen, and B. Li (2011), Minor stimulation of soil carbon storage by nitrogen addition: A meta-analysis, *Agr. Ecosyst. Environ.*, **140**, 234–244, doi:10.1016/j.agee.2010.12.010.
- Luo, Y., et al. (2011), Coordinated approaches to quantify long-term ecosystem dynamics in response to global change, *Global Change Biol.*, **17**, 843–854, doi:10.1111/j.1365-2486.2010.02265.x.
- Luo, Y., et al. (2012), A framework for benchmarking land models, *Biogeosciences*, **9**, 3857–3874, doi:10.5194/bg-9-3857-2012.
- Mao, J., L. Dan, B. Wang, and Y. Dai (2010), Simulation and evaluation of terrestrial ecosystem NPP with M-SDGVM over continental China, *Adv. Atmos. Sci.*, **27**, 427–442, doi:10.1007/s00376-009-9006-6.
- Mao, J., et al. (2015), Disentangling climatic and anthropogenic controls on global terrestrial evapotranspiration trends, *Environ. Res. Lett.*, **10**, 094008, doi:10.1088/1748-9326/10/9/094008.
- McGuire, A. D., et al. (2001), Carbon balance of the terrestrial biosphere in the twentieth century: Analyses of CO₂, climate and land use effects with four process-based ecosystem models, *Global Biogeochem. Cycles*, **15**, 183–206, doi:10.1029/2000GB001298.
- Meng, J., B. Wu, and Y. Zhou (2005), Monitoring terrestrial net primary productivity of China using BIOME-BGC model based on remote sensing, *IGARSS 2005: IEEE Int. Geosci. Remote Sens. Symp.*, **1–8**, 3105–3108.
- Mu, Q., M. Zhao, S. W. Running, M. Liu, and H. Tian (2008), Contribution of increasing CO₂ and climate change to the carbon cycle in China's ecosystems, *J. Geophys. Res.*, **113**, G01018, doi:10.1029/2006JG000316.
- Niu, S., et al. (2012), Thermal optimality of net ecosystem exchange of carbon dioxide and underlying mechanisms, *New Phytol.*, **194**, 775–783, doi:10.1111/j.1469-8137.2012.04095.x.

- Piao, S., J. Fang, and Q. Guo (2001), Terrestrial net primary production and its spatio-temporal patterns in China during 1982–1999, *Acta Sci. Nat. Univ. Pekin.*, *37*, 563–569.
- Piao, S., J. Fang, L. Zhou, B. Zhu, K. Tan, and S. Tao (2005), Changes in vegetation net primary productivity from 1982 to 1999 in China, *Global Biogeochem. Cycles*, *19*, GB2027, doi:10.1029/2004GB002274.
- Piao, S., J. Fang, P. Ciais, P. Peylin, Y. Huang, S. Sitch, and T. Wang (2009a), The carbon balance of terrestrial ecosystems in China, *Nature*, *458*, 1009–1013, doi:10.1038/nature07944.
- Piao, S., P. Ciais, P. Friedlingstein, N. de Noblet-Ducoudré, P. Cadule, N. Viovy, and T. Wang (2009b), Spatiotemporal patterns of terrestrial carbon cycle during the 20th century, *Global Biogeochem. Cy.*, *23*, GB4026, doi:10.1029/2008GB003339.
- Piao, S., et al. (2013), Evaluation of terrestrial carbon cycle models for their response to climate variability and to CO₂ trends, *Global Change Biol.*, *19*, 2117–2132, doi:10.1111/gcb.12187.
- Pierce, L. L., and S. W. Running (1995), The effects of aggregating sub-grid land surface variation on large-scale estimates of net primary production, *Landsc. Ecol.*, *10*, 239–253, doi:10.1007/BF00129258.
- R Core Team (2013), *R: A Language and Environment for Statistical Computing*, R Foundation for Statistical Computing, Vienna, Austria. [Available at <http://www.R-project.org/>]
- Ren, W., H. Tian, M. Liu, C. Zhang, G. Chen, S. Pan, B. Felzer, and X. Xu (2007), Effects of tropospheric ozone pollution on net primary productivity and carbon storage in terrestrial ecosystems of China, *J. Geophys. Res.*, *112*, D22509, doi:10.1029/2007JD008521.
- Richardson, A., D. Y. Hollinger, J. D. Aber, S. V. Ollinger, and B. H. Braswell (2007), Environmental variation is directly responsible for short- but not long-term variation in forest-atmosphere carbon exchange, *Global Change Biol.*, *13*, 788–803, doi:10.1111/j.1365-2486.2007.01330.x.
- Richmond, A., R. K. Kaufmann, and R. B. Myneni (2007), Valuing ecosystem services: A shadow price for net primary production, *Ecol. Econ.*, *64*, 454–462, doi:10.1016/j.ecolecon.2007.03.009.
- Rivington, M., K. B. Matthews, G. Bellocchi, and K. Buchan (2006), Evaluating uncertainty introduced to process-based simulation model estimates by alternative sources of meteorological data, *Agr. Syst.*, *88*, 451–471, doi:10.1016/j.agry.2005.07.004.
- Schimel, D., B. B. Stephens, and J. B. Fisher (2015), Effect of increasing CO₂ on the terrestrial carbon cycle, *Proc. Natl. Acad. Sci. U.S.A.*, *112*, 436–441, doi:10.1073/pnas.1407302112.
- Schuur, E. A., et al. (2015), Climate change and the permafrost carbon feedback, *Nature*, *520*, 171–179, doi:10.1038/nature14338.
- Schwalm, C. R., et al. (2010), A model-data intercomparison of CO₂ exchange across North America: Results from the North American Carbon Program site synthesis, *J. Geophys. Res.*, *115*, G00H05, doi:10.1029/2009JG001229.
- Schwalm, C. R., et al. (2015), Toward “optimal” integration of terrestrial biosphere models, *Geophys. Res. Lett.*, *42*, 4418–4428, doi:10.1002/2015GL064002.
- Shao, J., et al. (2015), Biotic and climatic controls on interannual variability in carbon fluxes across terrestrial ecosystems, *Agr. Forest Meteorol.*, *205*, 11–22, doi:10.1016/j.agrformet.2015.02.007.
- Sjögersten, S., C. R. Black, S. Evers, J. Hoyos-Santillan, E. L. Wright, and B. L. Turner (2014), Tropical wetlands: A missing link in the global carbon cycle?, *Global Biogeochem. Cycles*, *28*, 1371–1386, doi:10.1002/2014GB004844.
- Smith, N. G., and J. S. Dukes (2013), Plant respiration and photosynthesis in global-scale models: Incorporating acclimation to temperature and CO₂, *Global Change Biol.*, *19*, 45–63, doi:10.1111/j.1365-2486.2012.02797.x.
- Sun, R., and Q. Zhu (2000), Distribution and seasonal change of net primary productivity in China from April, 1992 to March, 1993, *Acta Geogr. Sin.*, *55*, 36–45.
- Tao, B., K. Li, X. Shao, and M. Cao (2003), Temporal and spatial pattern of net primary production of terrestrial ecosystems in China, *Acta Geogr. Sin.*, *58*, 372–380, doi:10.11821/xb200303006.
- Tao, F., and Z. Zhang (2010), Dynamic responses of terrestrial ecosystems structure and function to climate change in China, *J. Geophys. Res.*, *115*, G03003, doi:10.1029/2009JG001062.
- Therneau, T., B. Atkinson, and B. Ripley (2015), rpart: Recursive partitioning and regression trees, *R package version*, *4*, 1–10. [Available at <http://CRAN.R-project.org/package=rpart>]
- Tian, H., et al. (2011a), China's terrestrial carbon balance: Contributions from multiple global change factors, *Global Biogeochem. Cycles*, *25*, GB1007, doi:10.1029/2010GB003838.
- Tian, H., X. Xu, C. Lu, M. Liu, W. Ren, G. Chen, J. Melillo, and J. Liu (2011b), Net exchanges of CO₂, CH₄, and N₂O between China's terrestrial ecosystems and the atmosphere and their contributions to global climate warming, *J. Geophys. Res.*, *116*, G02011, doi:10.1029/2010JG001393.
- Tian, X., L. Shu, and M. Wang (2003), Direct carbon emissions from Chinese forest fires, 1991–2000, *Fire Saf. Sci.*, *12*, 6–10.
- Todd-Brown, K. E. O., J. T. Randerson, W. M. Post, F. M. Hoffman, C. Tarnocai, E. A. G. Schuur, and S. D. Allison (2013), Causes of variation in soil carbon simulations from CMIP5 Earth system models and comparison with observations, *Biogeosciences*, *10*, 1717–1736, doi:10.5194/bg-10-1717-2013.
- Turner, D. P., W. B. Cohen, and R. E. Kennedy (2000), Alternative spatial resolutions and estimation of carbon flux over a managed forest landscape in Western Oregon, *Landsc. Ecol.*, *15*, 441–452.
- Wang, H., X. He, and X. Zhang (2015), A comparative analysis of the post-2020 CO₂ emission reduction target set by China and the United States, *Chin. J. of Popul. Resour. Environ.*, *30*, 25–31.
- Wei, Y., et al. (2014), The North American Carbon Program (NACP) Multi-scale Synthesis and Terrestrial Model Intercomparison Project (MsTMIP): Part II – Environmental driver data, *Geosci. Model Dev.*, *7*, 2875–2893, doi:10.5194/gmd-7-2875-2014.
- Williams, C. A., N. P. Hanan, J. C. Neff, R. J. Scholes, J. A. Berry, A. S. Denning, and D. F. Baker (2007), Africa and the global carbon cycle, *Carbon Balance Manag.*, *2*, 3, doi:10.1186/1750-0680-2-3.
- Xiao, J., Q. Zhuang, E. Liang, A. D. McGuire, A. Moody, D. W. Kicklighter, X. Shao, and J. M. Melillo (2009), Twentieth-century droughts and their impacts on terrestrial carbon cycling in China, *Earth Interact.*, *13*, 10, doi:10.1175/2009EI275.1.
- Yan, Y., Y. Luo, X. Zhou, and J. Chen (2014), Sources of variation in simulated ecosystem carbon storage capacity from the 5th Climate Model Intercomparison Project (CMIP5), *Tellus B*, *66*, 22,568, doi:10.3402/tellusb.v66.22568.
- Yu, G., et al. (2013), Spatial patterns and climate drivers of carbon fluxes in terrestrial ecosystems of China, *Global Change Biol.*, *19*, 798–810, doi:10.1111/gcb.12079.
- Yu, G., et al. (2014), High carbon dioxide uptake by subtropical forest ecosystems in the East Asian monsoon region, *Proc. Natl. Acad. Sci. U.S.A.*, *111*, 4910–4915, doi:10.1073/pnas.1317065111.
- Yuan, W., et al. (2011), Thermal adaptation of net ecosystem exchange, *Biogeosciences*, *8*, 1453–1463, doi:10.5194/bg-8-1453-2011.
- Zaehle, S., and D. Dalmonech (2011), Carbon-nitrogen interactions on land at global scales: Current understanding in modeling climate biosphere feedbacks, *Curr. Opin. Environ. Sustain.*, *3*, 311–320, doi:10.1016/j.cosust.2011.08.008.
- Zhao, J., Y. He, Z. Li, and T. Yu (2012), China's sustainable forest management strategy under low-carbon economy, *World For. Res.*, *25*, 1–5.

- Zhou, L., X. Zhou, B. Zhang, M. Lu, Y. Luo, L. Liu, and B. Li (2014), Different responses of soil respiration and its components to nitrogen addition among biomes: A meta-analysis, *Global Change Biol.*, *20*, 2332–2343, doi:10.1111/gcb.12490.
- Zhou, X., Y. Fu, L. Zhou, B. Li, and Y. Luo (2013), An imperative need for global change research in tropical forests, *Tree Physiol.*, *33*, 903–912, doi:10.1093/treephys/tpt064.
- Zhu, W., Y. Pan, and J. Zhang (2007a), Estimation of net primary productivity of Chinese terrestrial vegetation based on remote sensing, *J. Plant Ecol.*, *31*, 413–424.
- Zhu, W., Y. Pan, X. Yang, and G. Song (2007b), Comprehensive analysis of the impact of climatic changes on Chinese terrestrial net primary productivity, *Chinese Sci. Bull.*, *52*, 3253–3260, doi:10.1007/s11434-007-0521-5.